TURUN YLIOPISTON JULKAISUJA
ANNALES UNIVERSITATIS TURKUENSIS

SARJA - SER. A I OSA - TOM. 396

ASTRONOMICA - CHEMICA - PHYSICA - MATHEMATICA

Discovery and Characterization of Na^+-Transporting Pyrophosphatases

by

Anssi Malinen

TURUN YLIOPISTO
Turku 2009

From the Department of Biochemistry and Food Chemistry
University of Turku
Turku, Finland

Supervised by

Professor Reijo Lahti, Ph.D.
Department of Biochemistry and Food Chemistry
University of Turku
Turku, Finland

and

Professor Alexander A. Baykov, Ph.D.
A.N. Belozersky Institute of Physico-Chemical Biology
Moscow State University
Moscow, Russia

Reviewed by

Professor Masayoshi Maeshima, Ph.D.
Graduate School of Bioagricultural Sciences
Nagoya University
Nagoya, Japan

and

Professor Mark S. Johnson, Ph.D.
Department of Biochemistry and Pharmacy
Åbo Akademi University
Turku, Finland

Opponent

Professor Aurelio Serrano, Ph.D.
Institute of Plant Biochemistry and Photosynthesis
University of Sevilla
Sevilla, Spain

ISBN 978-951-29-3913-8 (PRINT)
ISBN 978-951-29-3914-5 (PDF)
ISSN 0082-7002
Painosalama Oy – Turku, Finland 2009

To all curious people

CONTENTS

LIST OF ORIGINAL PUBLICATIONS **6**

ABSTRACT **7**

ABBREVIATIONS **9**

1 INTRODUCTION **10**

1.1 PP_i METABOLISM AND INORGANIC PYROPHOSPHATASES 10
1.2 THE PHYSIOLOGICAL FUNCTIONS OF H^+-PPASES 11
1.2.1 Distribution of H^+-PPases *11*
1.2.2 Subcellular localization of H^+-PPases *13*
1.2.3 H^+-PPase in plants *14*
1.2.4 H^+-PPase in protists *15*
1.2.5 H^+-PPase in prokaryotes *16*
1.2.6 H^+-PPase in stress response *17*
1.2.7 Effect of H^+-PPase overexpression on host cell phenotype *17*
1.3 STRUCTURE 18
1.3.1 Subunit composition *18*
1.3.2 Topological model *18*
1.3.3 Oligomeric structure *20*
1.3.4 A tentative evolutionary pathway to H^+-PPase structure *20*
1.4 ENZYMATIC PROPERTIES 21
1.4.1 Inhibitor sensitivity and turnover number *21*
1.4.2 K^+ dependence *21*
1.4.3 Mg^{2+} as cofactor *24*
1.4.4 pH dependence *25*
1.4.5 Synthesis of PP_i *25*
1.4.6 Transport activity *25*
1.5 EXPRESSION 27
1.6 PURIFICATION 28
1.7 FUNCTIONAL RESIDUES 29
1.7.1 Covalent inhibition *29*
1.7.2 Loops *30*
1.7.3 Residues affecting H^+ translocation *32*

2 AIMS OF THE STUDY **34**

3 METHODS **35**

3.1 SAMPLE PREPARATION 35
3.2 ASSAYS OF MEMBRANE PPASE ACTIVITIES 35
3.3 SEQUENCE AND DATA ANALYSIS 36

4 RESULTS AND DISCUSSION 36

4.1 DISCOVERY OF Na^+-TRANSPORTING PPASES (STUDIES II AND III) 36
4.1.1 Na^+-dependent membrane PPases 36
4.1.2 Transport specificity of Na^+-dependent membrane PPases 37
4.1.3 Subfamily of Na^+-transporting PPases 40
4.2 LIGAND BINDING IN Na^+-TRANSPORTING PPASES (STUDIES II, III, AND IV) 41
4.2.1 Scope 41
4.2.2 Mg^{2+} binding sites 41
4.2.3 Na^+ and K^+ binding sites 43
4.2.4 Interactions between ion binding sites 46
4.2.5 Conformational changes coupled to ligand binding 48
4.3 SITE-DIRECTED MUTAGENESIS OF RESIDUES UNIVERSALLY CONSERVED IN MEMBRANE PPASES (STUDY I) 51

ACKNOWLEDGMENTS 54

REFERENCES 55

REPRINTS OF ORIGINAL PUBLICATIONS 69

LIST OF ORIGINAL PUBLICATIONS

This thesis is based on the following publications, referred to in the text by Roman numerals:

I Malinen, A.M., Belogurov, G.A., Salminen, M., Baykov, A.A. and Lahti R. (2004) Elucidating the role of conserved glutamates in H^+-pyrophosphatase of *Rhodospirillum rubrum*. *J Biol Chem* **279**(26): 26811-26816.

II Belogurov, G.A., Malinen, A.M., Turkina M.V., Jalonen U., Rytkönen K., Baykov A.A. and Lahti, R. (2005) Membrane-bound pyrophosphatase of *Thermotoga maritima* requires sodium for activity. *Biochemistry* **44**(6): 2088-2096.

III Malinen A.M., Belogurov G.A., Baykov A.A. and Lahti, R. (2007) Na^+-pyrophosphatase: a novel primary sodium pump. *Biochemistry* **46**(30): 8872-8878.

IV Malinen A.M., Baykov A.A. and Lahti R. (2008) Mutual effects of cationic ligands and substrate on activity of the Na^+-transporting pyrophosphatase of *Methanosarcina mazei*. *Biochemistry* **47**(50): 13447-13454.

ABSTRACT

Proton pumping pyrophosphatase (H^+-PPase) is an integral membrane protein that utilizes the energy released upon hydrolysis of pyrophosphate (PP_i) to transport protons across the membrane against the electrochemical potential gradient. The first H^+-PPase was identified more than 40 years ago in the photosynthetic α-proteobacterium *Rhodospirillum rubrum*, and later also in the vacuolar membranes of land plants, acidocalcisomes of many free-living and parasitic protists, and cytoplasmic or endoplasmic membranes of some bacteria and archaea. In all H^+-PPase subcellular locations, the substrate-binding domain of the enzyme faces the cytoplasm. K^+-independent and K^+-dependent subfamilies of H^+-PPases are known. The subfamilies are closely related, but the latter enzymes require millimolar concentrations of K^+ for activity. Indeed, introduction of a Lys residue into the site specifically conserved as Ala in K^+-dependent H^+-PPases and Lys in K^+-independent enzymes abolished K^+-dependence of *Carboxydothermus hydrogenoformans* H^+-PPase. Physiologically, the function of H^+-PPase is most important during conditions of low energy and stress. Recently, H^+-PPase has emerged as a promising tool in plant engineering. Thus, overexpression of the enzyme in several agricultural plants has improved the survival of plants exposed to abiotic stresses such as drought, excessive salinity, and phosphorus limitation.

By the beginning of this study in 2002, sequencing projects had begun to yield fully sequenced prokaryotic genomes containing putative genes for H^+-PPases. We expressed the gene from a hyperthermophilic bacterium *Thermotoga maritima* in *Escherichia coli* and found the enzyme to be functionally novel in that Na^+ ions were absolutely required for activity. We later found similar Na^+-activated membrane PPases in the moderately thermophilic acetogenic bacterium *Moorella thermoacetica* and the Euryarchaeon *Methanosarcina mazei*. Surprisingly, instead of catalyzing H^+-transport inside *E. coli* inner membrane vesicles, the new Na^+-activated enzymes specifically transported Na^+ ions. PP_i-driven Na^+-transport was unaffected by the protonophore carbonyl cyanide *m*-chlorophenylhydrazone, inhibited by the Na^+ ionophore monensin, and activated by the K^+ ionophore valinomycin. Na^+ transport was accompanied by generation of a positive inside membrane potential, as reported by Oxonol VI probing. These findings defined a novel subfamily of membrane PPases acting as primary electrogenic Na^+ pumps; these are the Na^+-PPases.

Activities of Na^+-PPases displayed absolute requirements for both Mg^{2+} and Na^+, and were further activated by K^+. Detailed steady-state kinetic analysis of *M. mazei* Na^+-PPase (Mm-PPase) indicated that catalysis involved random-order binding of two Mg^{2+} ions and two Na^+ ions, and that binding was almost independent of substrate (Mg_2PP_i complex) attachment. Each pair of metal

ions, however, bound in a positively cooperative (or ordered) manner. This apparent cooperativity was lost only when Na^+ bound to preformed enzyme–Mg^{2+}–substrate complex. One of the Na^+ sites could also bind K^+, resulting in a 10-fold increase in the affinity of the other site for Na^+, and a 2.5-fold increase in all of maximal velocity, the Michaelis constant, and Mg^{2+}-binding affinity. To clarify the role of each ligand in permitting attainment of a conformation competent in catalysis, we determined the level of protection provided by each ligand against inactivation by the SH reagent mersalyl and protease trypsin. This revealed that Mg^{2+} ions play a crucial structural role in Mm-PPase. The successive binding of Mg_2PP_i and Na^+ induced a compact conformation of the enzyme cytoplasmic segment similar to that seen in the enzyme–phosphate product complex. Thus, the structure of Mm-PPase is flexible and may evolve cyclically in the course of catalytic turnover. Substitution of individual Asp residues in *T. maritima* Na^+-PPase suggested that Asp^{703} formed part of the Na^+ binding site but was not the sole determinant of Na^+-dependence.

In a separate study, we showed, using site-directed mutagenesis, that conserved Lys and Asp residues in cytoplasmic loops of *R. rubrum* H^+-PPase were functionally indispensable. In contrast, all Glu→Asp variants retained more than 30% of wild-type activity. However, the Glu→Asp variants displayed impaired catalytic efficiencies at low Mg^{2+} concentration. Substitution of Glu^{197}, Glu^{202}, or Glu^{649} resulted in decreased binding affinity for the substrate analogues aminomethylenediphosphonate and methylenediphosphonate, indicating that these residues are involved in substrate binding, acting as ligands for bridging metal ions. Following substitution of Glu^{550} and Glu^{649}, the enzyme was more susceptible to inactivation by mersalyl, suggesting a role for these residues in maintaining enzyme tertiary structure.

ABBREVIATIONS

AMDP	Aminomethylenediphosphonate
AMP	Adenosine monophosphate
AMS	4-acetamido-4'-maleimidylstilbene-2,2'-disulfonic acid
ADP	Adenosine diphosphate
ATP	Adenosine triphosphate
BM	3-(*N*-maleimidylpropionyl)biocytin
CBS	Cystathionine-beta-synthase
CCCP	Carbonyl cyanide *m*-chlorophenylhydrazone
Chaps	3-[(3-Cholamidopropyl)dimethylammonio]-1-propanesulfonate
DCCD	*N,N'*-dicyclohexylcarbodiimide
ena1	The gene encoding yeast plasma membrane Na^+-ATPase
H^+-PPase	Proton-translocating inorganic pyrophosphatase
Na^+-PPase	Sodium ion-translocating inorganic pyrophosphatase
IMV	Inner membrane vesicles
MEGA-9	Nonanoyl-*N*-methylglucamide
NEM	*N*-ethylmaleimide
P_i	Orthophosphate
PP_i	Inorganic pyrophosphate
PPase	Inorganic pyrophosphatase
Ch-PPase	*Carboxydothermus hydrogenoformans* inorganic pyrophosphatase
Mm-PPase	*Methanosarcina mazei* inorganic pyrophosphatase
Mt-PPase	*Moorella thermoacetica* inorganic pyrophosphatase
R-PPase	*Rhodospirillum rubrum* inorganic pyrophosphatase
Sc-PPase	*Streptomyces coelicolor* inorganic pyrophosphatase
Tm-PPase	*Thermotoga maritima* inorganic pyrophosphatase
TMS	Transmembrane segment
TRIS	Tris(hydroxymethyl)aminomethane
$\Delta G'$	Gibbs free energy under specified biochemical conditions
$\Delta\psi$	Membrane potential
$\Delta\mu_{H^+}$	Proton electrochemical potential gradient (proton-motive force)

1 INTRODUCTION

1.1 PP_i metabolism and inorganic pyrophosphatases

Inorganic pyrophosphate (PP_i) is a by-product of prominent nucleoside triphosphate-dependent biosynthetic reactions, including steps in nucleic acid, protein, polysaccharide, and lipid biosynthesis (Heinonen 2001). PP_i is produced in large quantities in actively growing cells, and PP_i turnover mediated by PP_i-utilizing enzymes provides an obligatory thermodynamic pull for various biosynthetic reactions. However, PP_i is also an energy-rich molecule and, under low energy conditions, cells may replace some ATP-dependent enzymes in metabolic pathways (for example glycolysis) with PP_i-dependent enzymes, to save biochemical energy (Huang *et al.* 2008). PP_i also regulates the activities of several enzymes and controls cellular processes such as calcification, cell proliferation, and iron transport. Abnormalities in PP_i metabolism are linked to various diseases (Heinonen 2001).

In the majority of living species, divalent metal ion-dependent inorganic pyrophosphatases (PPases; EC 3.6.1.1) hydrolyse the bulk of the PP_i pool to orthophosphate (P_i). Three families of structurally and evolutionarily unrelated PPases have been identified to date (Shintani *et al.* 1998; Young *et al.* 1998; Baykov *et al.* 1999; Serrano *et al.* 2007). The members of two soluble PPase families (families I and II) dissipate the energy of PP_i as heat, whereas membrane-bound PPases are primary proton pumps that save part of the free energy from PP_i hydrolysis ($\Delta G' \approx -17$ kJ mol^{-1} *in vivo*; (Heinonen 2001)) in the form of proton gradients. Family I PPases are most widespread. Family II enzymes are restricted to some prokaryotic species (Jämsén *et al.* 2007), and H^+-transporting PPases (H^+-PPases) are sporadically distributed across the tree of life (Belogurov 2004; Serrano *et al.* 2007).

The importance of PPases and PP_i metabolism is reinforced by the multitude of mechanisms that organisms employ to regulate the synthesis and activity of PPases. For example, the expression of family I PPases is up-regulated in response to a broad spectrum of stress conditions, such as salt stress in barley (Ueda *et al.* 2006), cold in wheat (Gulick *et al.* 2005), calorie restriction in cows (Kuhla *et al.* 2007), phosphate deprivation in bacteria (Gomez-Garcia *et al.* 2003), and in human cancer tissues (Chen *et al.* 2002; Lexander *et al.* 2005). Inhibition of the catalytic activities of family I PPases by phosphorylation appears, however, to form part of the mechanism preventing self-fertilization in the field poppy flower (de Graaf *et al.* 2006). The role of phosphorylation in regulation of *Streptococcus agalactiae* family II PPase remains unknown (Rajagopal *et al.* 2003), but another regulatory mechanism has been discovered in some family II enzymes, which harbor cystathionine-beta-synthase (CBS) domains absent in other family II enzymes. In these

enzymes, CBS domains bind AMP, ADP, and ATP, affording allosteric control of PPase activity (Jämsén *et al.* 2007). As with the soluble PPases, H^+-PPases are regulated at both the gene and protein level (see below).

This doctoral thesis focuses on H^+-PPases, which constitute a distinct class of ion translocases with no apparent sequence similarities to ubiquitous ATP-powered pumps, such as F-, V-, or P-type ATPases or ABC transporters. H^+-PPases can be divided into two functionally divergent and independently evolving subfamilies (Perez-Castineira *et al.* 2001; Belogurov and Lahti 2002a). The enzymes of the K^+-dependent subfamily require millimolar concentrations of K^+ for maximal activity, whereas K^+-independent subfamily members have no such requirement. In this section, I review available information on the physiology and enzymology of H^+-PPases. In the later parts of the thesis, the focus shifts to our original contributions to the field. The core new finding of the thesis is the discovery of Na^+-transporting PPases, which constitute a novel subfamily of membrane PPases.

1.2 The physiological functions of H^+-PPases

1.2.1 Distribution of H^+-PPases

Baltscheffsky and Baltscheffsky first reported energy-linked PP_i synthesis and hydrolysis activities in a cytoplasmic membrane preparation (chromatophores) of the photosynthetic bacterium *R. rubrum* (Baltscheffsky *et al.* 1966; Baltscheffsky 1967). Further studies indicated that PPase functioned as an H^+ transporter (Moyle *et al.* 1972). Almost a decade later, H^+-transporting PPase activities were found in plant membrane preparations, extending enzyme distribution to eukaryotes (Karlsson 1975; Walker and Leigh 1981; Chanson *et al.* 1985; Rea and Poole 1985). More recently, H^+-PPases have been found in several parasitic protists (Scott *et al.* 1998; Luo *et al.* 1999; Rodrigues *et al.* 1999a,b; Drozdowicz and Rea 2001) and the archaeon *Pyrobaculum aerophilum* (Drozdowicz *et al.* 1999), demonstrating the deep phylogenetic roots of the enzyme.

In the genomic era, the availability of H^+-PPase gene sequences has increased exponentially and database searches confirm the wide distribution of the enzyme (Table 1). In the Archaean domain, the enzyme is evident among Crenarchaeota, Euryarchaeota, and Korarchaeota, whereas half of the Bacteria classes include H^+-PPase host species. The wide span of physico-chemical environments colonized by host organisms, and diversities in the metabolic strategies of H^+-PPase-hosting life forms (Serrano *et al.* 2004), indicates significant adaptability in H^+-PPase structure and function. Among eukaryotes, H^+-PPase has been identified in vacuolar membranes from all major vascular plant types (monocotyledons, dicotyledons, C3, C4, and CAM plants)

(Karlsson 1975; Walker and Leigh 1981; Wanger and Mulready 1983; Chanson *et al.* 1985; Rea and Poole 1985; Rea and Poole 1986; Wang *et al.* 1986), as well as their possible ancestors, the charophyte algae (Shimmen and MacRobbie 1987), and the unicellular marine alga *Acetabularia mediterranea* (Ikeda *et al.* 1991). H^+-PPase is also common among diverse free-living and parasitic protists (Perez-Castineira *et al.* 2002a), but has not been identified in fungi. Interestingly, an H^+-PPase polypeptide and enzyme activity have been reported in yolk ovarian tissue granules of the insect *Rhodnius prolixus* (Motta *et al.* 2004) and the domestic cockroach *Periplaneta americana* (Motta *et al.* 2009), both of which are vectors for pathogenic protists. These findings would extend H^+-PPase distribution to the animal world, but further work on H^+-PPase genes in animal genomes is required, to exclude the possibility that the enzymes detected were encoded by carried protists.

Table 1. The distribution of H^+-PPases [a].

Archaea	**Bacteria**	**Eukaryotes**
+ Crenarchaeota	+ Actinobacteria	+ Alveolata
+ Euryarchaeota	- Aquificae	+ Amoebozoa
+ Korarchaeota	+ Bacteroidetes / Chlorobi	- Apusozoa
- Nanoarchaeota	+ Chlamydiae / Verrucomicrobia	- Centroheliozoa
	+ Chloroflexi	+ Cryptophyta
	- Chrysiogenetes	- Diplomonadida
	- Cyanobacteria	+ Euglenozoa
	- Deferribacteres	- Fungi / Metazoa
	- Deinococcus-Thermus	- Glaucocystophyceae
	+ Dictyoglomi	+ Haptophyceae
	- Fibrobacteres / Acidobacteria	- Heterolobosea
	+ Firmicutes	- Jakobida
	+ Fusobacteria	- Katablepharidophyta
	- Gemmatimonadetes	- Malawimonadidae
	- Nitrospirae	- Nucleariidae
	+ Planctomycetes	- Oxymonadida
	+ Proteobacteria	- Parabasalidea
	+ Spirochaetes	+ Rhizaria
	- Synergistetes	+ Rhodophyta
	- Tenericutes	+ Stramenopiles
	- Thermodesulfobacteria	+ Viridiplantae
	+ Thermotogae	

[a] The presence or absence of H^+-PPase genes in any phylogenetic class is indicated by + and - signs, respectively. The terminology is that of the National Center for Biotechnology Information (Bethesda, MD; http://www.ncbi.nlm.nih.gov/Taxonomy/). Genes were detected as hits in a BLAST search (Altschul *et al.* 1990) of non-redundant protein sequences, in January 2009, using *R. rubrum* H^+-PPase as the query protein sequence.

The distribution of H^+-PPase is not only wide but also sporadic. For example, in the Bacteria domain the spirochaetes *Treponema denticola* and *Leptospira interrogans* have genes encoding H^+-PPases, whereas *Treponema pallidum* and *Borrelia burgdoferi* do not. Similarly, the firmicutes *Clostridium tetani* and *Clostridium thermocellum* have H^+-PPase genes, but not the closely related *Clostridium perfringens* or *Clostridium acetobutylicum*. H^+-PPase-encoding

sequences appear ubiquitous in alphaproteobacteria but are absent from the order Rickettsiales. Thus, H^+-PPase genes have a high propensity for lineage-specific loss and/or lateral transfer. The genomes of methanogenic archeae from the Methanosarcina order, the bacterium *Dehalococcoides ethenogenes*, the plant *Arabidopsis thaliana*, and protists from the Plasmodium order contain two divergent genes encoding H^+-PPase, signifying that H^+-PPases do not represent a homogenous family of orthologs, but comprise at least two subfamilies of paralogous genes (Belogurov 2004).

With few exceptions, sequenced genomes containing H^+-PPases additionally include genes for soluble PPases. Family I PPase is the most frequent companion of H^+-PPase. Whereas genes for an ordinary family II PPase and H^+-PPase have not been detected in the same organism, enzymatically less active family II PPases containing regulatory CBS-domains seem to be compatible with H^+-PPases (Jämsén *et al.* 2007). Overall, the data imply that species rarely, if ever, rely on H^+-PPase as the sole PP_i disposal system; other PP_i-consuming enzymes are present. However, H^+-PPase is able to functionally complement a conditional soluble PPase deficiency in *Saccharomyces cerevisiae* under laboratory conditions (Perez-Castineira *et al.* 2002b), reinforcing the hypothesis that both H^+-PPases and soluble PPases may be responsible for PP_i turnover, during different phases of the life cycle or in specific cellular compartments.

1.2.2 Subcellular localization of H^+-PPases

Recently, acidocalcisome-associated H^+-PPase activities have been discovered in evolutionarily diverse organisms such as bacteria (Seufferheld *et al.* 2003; Seufferheld *et al.* 2004), protists (Scott *et al.* 1998; Luo *et al.* 1999; Drozdowicz *et al.* 2003), and algae (Ruiz *et al.* 2001). Several reports also indicate that H^+-PPase is present in the Golgi apparatus and plasma membrane of plants and protists (Oberbeck *et al.* 1994; Long *et al.* 1995; Robinson *et al.* 1996; Robinson *et al.* 1998; Ratajczak *et al.* 1999; McIntosh *et al.* 2001; Mitsuda *et al.* 2001; Martinez *et al.* 2002). The detection of H^+-PPase in the Golgi may be a consequence of trafficking, but it is likely that the traditional view that H^+-PPase localizes exclusively in the plasma membrane in prokaryotes and the vacuolar membrane in plants is overly simplistic. Rather, H^+-PPase appears to distribute between the plasma membrane and the membranes of organelles. In plants, the relevant organelles are primarily vacuoles, but acidocalcisomes of protists and bacteria contain the enzyme. Independent of subcellular localization, the substrate-binding domain of the enzyme always faces the cytoplasm.

1.2.3 H^+-PPase in plants

The role of plant H^+-PPases as proton pumps, sharing responsibility with vacuolar-type H^+-ATPases to maintain proton gradients across the vacuolar membrane, is firmly established (Maeshima 2000; Drozdowicz and Rea 2001). A proton gradient thus created is the driving force for secondary transporters that accumulate various solutes, such as ions and sugars, inside the vacuole. Each vacuole is a large storage organelle typically filling at least 50% of total cell volume and has a pivotal role in controlling intracellular osmotic pressure and cell expansion, for example during fruit ripening (Martinoia *et al.* 2007). The relative contributions of H^+-PPase and H^+-ATPase to vacuole acidification depends on the growth phase. H^+-PPase protein level and activity tend to be highest in young actively growing plant tissue, whereas the contribution of H^+-ATPase becomes dominant in fully developed tissue (Suzuki and Kasamo 1993; Shiratake *et al.* 1997; Facanha and de Meis 1998; Nakanishi and Maeshima 1998). In growing tissue, nucleotide triphosphate-dependent reactions produce large amounts of PP_i, which H^+-PPases and/or soluble PPases recycle to P_i to prevent thermodynamic inhibition of biosynthetic pathways. For example, the *in vitro* biosynthetic yield of rubber decreased fourfold when the H^+-PPase of rubber tree particles was inhibited (Zeng *et al.* 2009). Also, by relying on H^+-PPase for ΔpH maintenance in vacuoles and possibly other organelles, the growing plant cell can channel the nucleotide triphosphate pool for promotion of biosynthetic reactions. As the tissue matures, the demand for biochemical energy decreases, and it may become more economical for the cell to constrain H^+-PPase expression.

In addition to a role as a vacuolar energy saver, H^+-PPase may function in regulation of plant growth and development. Overexpression of H^+-PPase in *Arabidopsis thaliana* (ecotype Col-0) resulted in increased cell division at the onset of organ formation, and hyperplasia (Li *et al.* 2005)(Fig. 1). Hyperplasia, most significantly in the root system, has also been also observed in tomato (Park *et al.* 2005), tobacco (Gao *et al.* 2006), cotton (Lv *et al.* 2008), and maize (Li *et al.* 2008), and therefore appears to be a general consequence of H^+-PPase overexpression in plants. Disruption of the major H^+-PPase genes (AVP1) in *Arabidopsis* species, in contrast, impeded root and shoot development (Li *et al.* 2005)(Fig. 1), although the developmental defect severities depended on the *Arabidopsis* ecotype (Gaxiola *et al.* 2007). The expression level of H^+-PPase correlated with root tip levels of the growth-promoting hormone auxin (Li *et al.* 2005). However, the total amount of auxin was unaffected, indicating that changes in local auxin concentrations were consequences of redistribution and enhanced transport of the existing auxin pool. Because auxin is a weak acid (pK_a 4.75), the ΔpH across the plasma membrane effectively controls diffusion-based hormone uptake by the cell, as well as hormone efflux (Lomax *et al.* 1985). H^+-PPase overexpression increased ΔpH in the roots of gain-of-

function mutant plants promoting cellular uptake of the protonated, lipophilic, form of auxin. The opposite effect was observed in H^+-PPase loss-of-function mutants. H^+-PPase level further correlated with the level of P-type H^+-ATPase in the plasma membrane, suggesting that the effect of H^+-PPase expression on the observed ΔpH could be indirect, and arise from the participation of H^+-PPase located in the Golgi apparatus and endosomes to the trafficking of H^+-ATPase to the plasma membrane (Li *et al.* 2005).

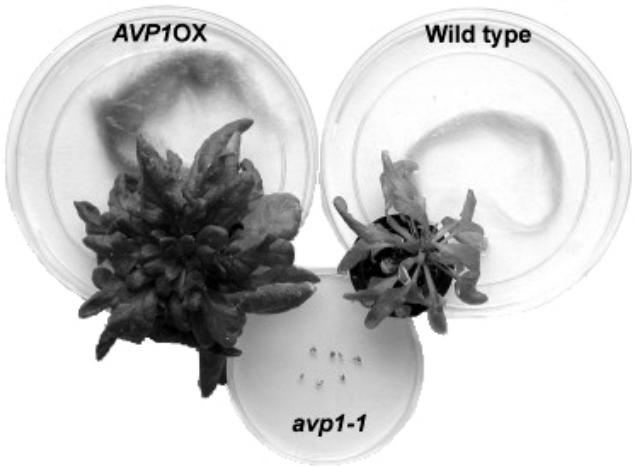

Figure 1. Phenotypes of gain- (*AVP1OX*) and loss-of-function (*avp1-1*) H^+-PPase mutants of *A. thaliana* (Gaxiola *et al.* 2007).

1.2.4 H^+-PPase in protists

Most information on physiological functions of H^+-PPases in protozoa comes from studies of pathogenic parasites in the groups Trypanosoma, Plasmodium, and Toxoplasma. These unicellular protozoa have diverse life cycles including transmission from one host organism to another (*e.g.,* from mosquito to human), and dwell in host extracellular environments before invading cells to initiate proliferation. Organisms encountering such diverse environments and stresses have quite likely benefited from use of the PP_i-dependent energy-saving system during evolution, especially because parasitic protists gain metabolic energy principally by fermenting sugars, which results in only modest ATP yields.

H^+-PPase appears to be expressed through the entire life cycle of the parasite (Scott *et al.* 1998; Rodrigues *et al.* 1999a). The enzyme is most abundant in the membranes of acidocalcisomes but localizes also to the plasma membrane and the membranes of other cell organelles. Although H^+-PPase contributes, together with H^+-ATPase, to proton pumping in all membranes where the enzyme is found, H^+-PPase function in acidocalcisomal membranes appears to be of most significance. In the absence of H^+-PPase, acidocalcisomes lose acidity, their polyphosphate content, and the ability to release Ca^{2+} ions

(Lemercier *et al.* 2002). Impairment of acidocalcisome function has detrimental effects on pH and ion homeostasis, osmotic regulation, and parasite growth rate (Lemercier *et al.* 2002; Fang *et al.* 2007). Although the defects are usually not lethal under laboratory conditions, a mutant parasite displaying alterations in H^+-PPase trafficking and activity failed to establish an infection in the mouse (Besteiro *et al.* 2008). In addition, several PP_i-analogues inhibiting H^+-PPase activity *in vitro* retarded the growth of parasitic protists in cell and animal models (Urbina *et al.* 1999; Rodrigues *et al.* 2000; McIntosh *et al.* 2001; Drozdowicz *et al.* 2003). Some of these compounds, however, target additional enzymes *in vivo* (Docampo and Moreno 2008), making it difficult to use PP_i-analogue administration to define the contribution of H^+-PPase to protist fitness inside host organisms.

1.2.5 H^+-PPase in prokaryotes

The purple nonsulfur photosynthetic bacterium *R. rubrum* has served as a model system in studies exploring the physiological function of H^+-PPase in prokaryotes. *R. rubrum* is metabolically versatile, being able to proliferate using anaerobic photosynthesis, aerobic or anaerobic respiration, or fermentation (Schultz and Weaver 1982). Under anaerobic conditions, H^+-PPase is expressed throughout all growth phases in both photosynthetic and fermentative cultures (Lopez-Marques *et al.* 2004), but the expression level declines progressively in transition to aerobic conditions (Romero *et al.* 1991; Lopez-Marques *et al.* 2004; Seufferheld *et al.* 2004). Disruption of the H^+-PPase gene yielded a mutant strain able to grow normally, using anaerobic photosynthesis, under high-intensity light (21 W/m^2), but showing a long delay prior to proliferation at intermediate light levels (3.6–6.3 W/m^2), and that failed to grow altogether at low light intensity (2 W/m^2) (Garcia-Contreras *et al.* 2004). Under aerobic conditions, the mutant proliferated normally at high oxygen pressure (21%) but showed a prolonged lag and a decreased growth rate at lower oxygen pressure (10%).

These data suggest that H^+-PPase is important for the growth of *R. rubrum* under low-energy conditions, such as in the dark or during anoxia, and the enzyme also plays an important role in metabolic transitions (Garcia-Contreras *et al.* 2004; Lopez-Marques *et al.* 2004). During transitions, H^+-PPase probably hydrolyses PP_i to enhance the proton-motive force, which the bacterium uses to promote various metabolic functions. As the energy supply of the cell improves and the electron transport chain creates a stronger proton-motive force, H^+-PPase is no longer needed to sustain growth. It has been hypothesized (Nyren and Strid 1991) that under these conditions H^+-PPase in respiratory or photosynthetic membranes reverses its action and begins to synthesize PP_i in conjunction with downhill proton translocation. Indeed, *R. rubrum* H^+-PPase is able to synthesize PP_i at a significant rate in isolated, energized

chromatophores (Baltscheffsky *et al.* 1966; Baltscheffsky 1967; Guillory and Fisher 1972; Moyle *et al.* 1972; Nyren *et al.* 1986). However, a more recent report indicated that rather than being restricted to the photosynthetic chromatophore membrane, the enzyme localizes predominantly to acidocalcisomes devoid of known enzymatic systems promoting a proton-motive force sufficiently great to energize PP_i synthesis (Seufferheld *et al.* 2004). In addition, the bacterium downregulates H^+-PPase expression under high-energy growth conditions (aerobiosis) (Lopez-Marques *et al.* 2004).

1.2.6 H^+-PPase in stress response

Organisms possessing H^+-PPase genes tend to frequently encounter environmental conditions severely constraining cell energy status. Exposure of plants to anoxia, cold, drought, salt, or nutrient scarcity increased the abundances and activities of H^+-PPases (Colombo and Cerana 1993; Zingarelli *et al.* 1994; Carystinos *et al.* 1995; Ballesteros *et al.* 1996; Palma *et al.* 2000; Fukuda *et al.* 2004; Yang *et al.* 2007). H^+-PPase was similarly salt-inducible in the bacterium *R. rubrum* (Lopez-Marques *et al.* 2004). The H^+-PPase response is coordinated with regulation of other host cell anti-stress machinery components. In plants, H^+-PPase is often congruently regulated with vacuolar H^+-ATPase and the Na^+/H^+ antiporter reflecting the importance of effective vacuolar energization and Na^+ sequestration in survival during stress. The general stress hormone abscisic acid (Fukuda and Tanaka 2006), and the nitric oxide signaling pathway (Zhang *et al.* 2006), may trigger the vacuolar protein response. Salt-stressed *R. rubrum*, on the other hand, appeared to employ alternative stress response-linked sigma factors to enhance expression of H^+-PPase and other proteins (Lopez-Marques *et al.* 2004). H^+-PPase therefore seems to have a universal stress protection function. However, H^+-PPase may facilitate organism fitness during stress by several mechanisms. The plasma membrane-localized enzyme may provide a proton-motive force for ATP synthesis, whereas H^+-PPase in the acidocalcisomes is the primary enzyme responsible for maintaining organ acidity and functionality. Acidocalcisomes appear to be the main organ involved in polyphosphate metabolism, and have been suggested to play crucial roles in a plethora of stress responses (Docampo *et al.* 2005; Seufferheld *et al.* 2008).

1.2.7 Effect of H^+-PPase overexpression on host cell phenotype

Diverse model and agricultural plants have been engineered to overexpress H^+-PPases. In comparison to wild-type strains, transgenic *A. thaliana* (Gaxiola *et al.* 2001; Guo *et al.* 2006), tomato (Park *et al.* 2005), tobacco (D'yakova *et al.* 2006; Gao *et al.* 2006), rice (Zhao *et al.* 2006), maize (Li *et al.* 2008), and cotton (Lv *et al.* 2008) were notably salt- and drought-tolerant. The mutant plants also outperformed controls when grown with limited phosphorus (Yang *et al.* 2007). Similar phenotypes resulted from overexpression of bacterial or

plant H^+-PPase genes. Two factors likely contribute to enhanced stress tolerance. First, plant strains overproducing H^+-PPase develop bigger and more robust root systems, obviously beneficial under conditions of high salinity and drought (Fig. 1)(Li *et al.* 2005; Lv *et al.* 2008). Second, increased H^+-PPase activity in the vacuolar membrane provides a stronger proton-motive force driving vacuolar ion sequestration. This allows the plant to avoid the toxic effects of cytoplasmic ions such as Na^+ and Cl^-, and to better maintain the osmotic potential required to drive water uptake into cells. In accordance with this model, higher proton-motive forces and Na^+ concentrations have been measured in vacuoles isolated from transgenic plant cells (Duan *et al.* 2007). Transgenic plants also accumulated more Na^+ and K^+ in root and leaf tissues (Gaxiola *et al.* 2001; Lv *et al.* 2008).

Overexpression of *A. thaliana* H^+-PPase conferred salt tolerance on the salt-sensitive *ena1* mutant of *S. cerevisiae* (Gaxiola *et al.* 1999). Suppression of salt sensitivity required two ion transporters, specifically the Cl^- channel and the Na^+/H^+ antiporter. Additionally, H^+-PPases of *A. thaliana* and *Chloroflexus aurantiacus* expressed from autonomous plasmids functionally complemented soluble PPase deficiency (Perez-Castineira *et al.* 2002b).

1.3 Structure

1.3.1 Subunit composition

Purified H^+-PPase preparations from native bacterial or plant sources migrate as a single band in sodium dodecyl sulfate polyacrylamide gel electrophoresis (Nyren *et al.* 1984; Britten *et al.* 1989; Maeshima and Yoshida 1989). When purified polypeptides are reconstituted into liposomes, they were able to translocate protons (Shakhov *et al.* 1982; Sato *et al.* 1994). The expression in *S. cerevisiae* of cDNA encoding the substrate-binding subunit of *A. thaliana* H^+-PPase resulted in expression of an enzyme active in PP_i-hydrolysis and H^+-transport (Kim *et al.* 1994). The heterologously expressed pump was indistinguishable from the native plant enzyme in terms of cofactor dependence, inhibitor sensitivity, and immunological reactivity. Evidence from purification and expression studies thus unambiguously establishes that H^+-PPase is composed of a single polypeptide. Thus, the molecular architecture of H^+-PPase is one of the simplest among ion pumps.

1.3.2 Topological model

The membrane topology of *Streptomyces coelicolor* H^+-PPase (Sc-PPase) expressed in *E. coli* has been experimentally determined by cysteine-scanning analysis. Mimura and colleagues (Mimura *et al.* 2004) first engineered a cysteine-free enzyme and then introduced single cysteines in 42 sites locating in computationally predicted hydrophilic loops. The orientations of the

introduced cysteines in variant Sc-PPases were determined by sequentially incubating intact *E. coli* cells with the membrane-impermeable cysteine probe AMS (4-acetamido-4'-maleimidylstilbene-2,2'-disulfonic acid) and the biotinylated membrane-permeable probe BM [3-(*N*-maleimidylpropionyl)biocytin] (Fig. 2). AMS markedly reduced the cysteine biotinylation in 11 variants (S7C, T15C, Q96C, D187C, D281C, T352C, S360C, S443C, T552C, L652C, and S746C), indicating that these residues are exposed to the periplasm. Biotinylation of the other 16 residues was not affected by AMS treatment, indicating that cysteine residues in those variants (S52C, I56C, T137C, S151C, F213C, I231C, T241C, S313C, A317C, T391C, S485C, T497C, I605C, T700C, T705C, and S787C) face the cytoplasm. Finally, nine variants (S101C, V183C, C253C, S282C, R308C, L438C, S545C, S740C, and S768C) did not react with BM, even in the absence of AMS, indicating that these residues were located in transmembrane segments or otherwise buried in the structure.

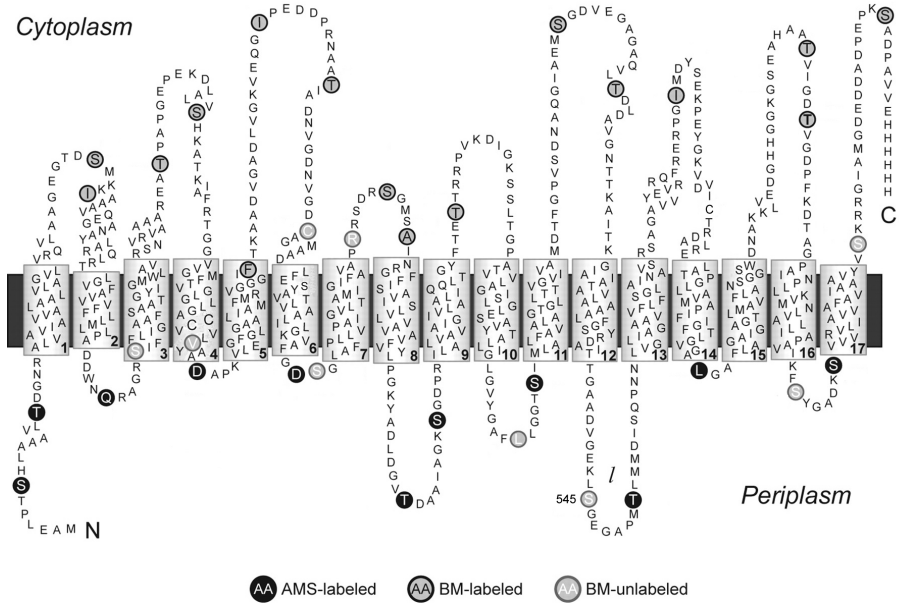

Figure 2. The topological model of *S. coelicolor* H^+-PPase (Mimura *et al.* 2004). The transmembrane segments of Sc-PPase were predicted using the TMHMM program (Krogh *et al.* 2001). Amino acid positions accessible from the periplasm or cytoplasm are indicated using black and grey circles, respectively. Inaccessible residues are depicted as white letters in grey circles. Ser^{545} is numbered. The six His residues at the C-terminus are a His tag.

The distances between introduced cysteines were sufficient to permit only a single traverse of the membrane, and the cysteine-labeling data thus allowed enzyme membrane topology to be determined (Fig. 2). According to the model (Mimura *et al.* 2004), Sc-PPase contains 17 transmembrane segments. The N-terminal end of the polypeptide faces the periplasm, whereas the C-terminus is

in the cytoplasm. Importantly, Sc-PPase has a long C-terminal extension that does not align with the majority of H^+-PPase sequences. This extension contains an extra transmembrane segment, signifying that the core H^+-PPase structure consists of only 16 transmembrane segments. N-terminal polypeptide extensions in some other H^+-PPases may also contain additional transmembrane segments.

1.3.3 Oligomeric structure

Chemical cross-linking, gel filtration, and electron microscopic studies of membrane-bound or purified H^+-PPases are consistent with association of two identical subunits in a dimer complex (Maeshima 1990; Nyren *et al.* 1991; Sato *et al.* 1991; Tzeng *et al.* 1996; Yang *et al.* 1998; Lopez-Marques *et al.* 2005). The dimer interface is probably located near Ser^{545} in the periplasmic loop *l* of Sc-PPase, because Cys in this position formed an intermonomer disulfide bridge (Mimura *et al.* 2005b). Cross-linking of double Cys variants also trapped higher molecular mass complexes, suggesting that two or three individual dimers may, at least transiently, associate to higher order oligomers (Mimura *et al.* 2005b).

Several lines of evidence suggest that the physical interaction of H^+-PPase subunits in the dimer has functional consequences. First, radiation inactivation studies indicated the minimal unit for proton transport to be a dimer (Wu *et al.* 1991; Tzeng *et al.* 1996) or tetramer (Sarafian *et al.* 1992b). Second, the activity (Mimura *et al.* 2005b) and thermal stability (Yang *et al.* 2004) of a functional subunit appeared reduced when complexed with a non-functional subunit. Third, and more controversially, some radiation inactivation studies have estimated the functional size for PP_i hydrolysis activity to be the dimer (Sato *et al.* 1991; Wu *et al.* 1991; Tzeng *et al.* 1996), but other studies have identified the monomer as active (Sarafian *et al.* 1992b; Fraichard *et al.* 1993). Thus, a single catalytic subunit may be insufficient, at least for H^+ translocation activity.

1.3.4 A tentative evolutionary pathway to H^+-PPase structure

The N-terminal, central, and C-terminal thirds of H^+-PPase polypeptides show statistically significant similarities in amino acid sequence and distribution of hydrophobic and amphipathic segments (Au *et al.* 2006). Au and co-workers (Au *et al.* 2006) therefore suggested that the N-terminal fragment, including transmembrane segments 1–6 (TMS 1–6), was triplicated in the H^+-PPase ancestor. The central repetitive unit in the resulting 18-TMS polypeptide would subsequently have lost the fragment corresponding to the original TMS 5–6 yielding the current, tripartite, pseudo-symmetrical 6 TMS–4 TMS–6 TMS polypeptide. In such a structure, elements of the three repeat units could provide the equivalent of an oligomeric H^+-channel often observed in channel-

forming peptides and proteins (Saier 2003). It has also been argued that the H^+-PPase protein family is very old and represents a molecular fossil from a possible era of PP_i-dependent energy metabolism pre-dating the rise of ATP-dependent bioenergetics (Baltscheffsky *et al.* 1999; Hedlund *et al.* 2006).

1.4 Enzymatic properties

1.4.1 Inhibitor sensitivity and turnover number

In complex biological samples, both soluble PPase and H^+-PPase activities are commonly present. The activities of the two enzymes can, however, be isolated, based on different inhibition susceptibilities to fluoride and the PP_i analogue aminomethylenediphosphonate (AMDP) (Baykov *et al.* 1993a). Fluoride is a weak inhibitor of H^+-PPases (K_i values of 4.8 mM and 3.4 mM for *R. rubrum* and *A. thaliana* H^+-PPase, respectively (Baykov *et al.* 1993a)) but a strong inhibitor of soluble PPases (K_i values of 90 μM for *E. coli* PPase (Kurilova *et al.* 1984) and ≤10 μM for *S. cerevisiae* PPase (Baykov *et al.* 2000)). Thus, addition of 250–500 μM fluoride specifically eliminates the soluble PPase contribution to observed PP_i hydrolysis. Conversely, only H^+-PPases are readily inhibited by AMDP, which has K_i values of less than 2 μM against *R. rubrum* and plant H^+-PPases (Baykov *et al.* 1993a; Zhen *et al.* 1994a), but K_i values at least an order of magnitude higher against soluble PPases (Smirnova *et al.* 1988; Zhen *et al.* 1994a). Other 1,1-diphosphonates, such as hydroxymethylenediphosphonate and its aminomethyl derivative (H_2N-CH_2-$C(PO_3)_2$-OH), act as competitive inhibitors of H^+-PPases, but show less affinity and specificity (Baykov *et al.* 1993a; Gordon-Weeks *et al.* 1999).

The turnover numbers (k_{cat} values) of H^+-PPases, as calculated from reported specific PP_i hydrolysis rates, are 10–20 s^{-1} (at 25–30°C) for enzymes purified from plant vacuoles (Maeshima and Yoshida 1989; Sato *et al.* 1994; Suzuki *et al.* 1999). The k_{cat} value of the *R. rubrum* enzyme is slightly higher (24 s^{-1} at 20°C) (Nyren *et al.* 1991), and that of the hyperthermophilic *T. maritima* enzyme expressed and purified from yeast is lower (6 s^{-1} at 70°C) (Lopez-Marques *et al.* 2005). Notably, all purified H^+-PPases require lipids to attain maximal apparent activities. As with purified enzymes, the k_{cat} value of membrane-bound, crude, *V. radiata* H^+-PPase was estimated by patch-clamp analysis to be 14 s^{-1} (at 25°C) (Nakanishi *et al.* 2003).

1.4.2 K^+ dependence

The existence of K^+-dependent and K^+-independent H^+-PPases has been known for some time (Baltscheffsky *et al.* 1966; Karlsson 1975; Walker and Leigh 1981). K^+-independent H^+-PPases are insensitive to monovalent cations, whereas K^+-dependent enzymes require millimolar concentrations of K^+ for activity. Structurally similar ions, such as Rb^+, Cs^+, NH_4^+, Na^+, and Li^+, are

able to substitute for K^+, the physiological activator, to variable degrees (Gordon-Weeks *et al.* 1997). K^+ binding occurs from the cytoplasmic side of the membrane (Davies *et al.* 1991) and kinetic modeling of the dependence of hydrolytic activity rate on K^+ concentration suggested the presence of a single K^+ binding site in each K^+-dependent H^+-PPase (Baykov *et al.* 1993b). Reported K_d values for K^+ activation vary significantly, from less than 4 mM to over 60 mM (Walker and Leigh 1981; Rea and Poole 1985; Wang *et al.* 1986; Baykov *et al.* 1993b). This variation most likely arises because buffer cations vary in different reports; these cations interact with K^+ binding sites and inhibit enzymatic activity in the following order: Tris > Bis-Tris-propane > Bicine = Tricine > imidazole. When buffer effects on K^+ binding and maximal catalytic rates are considered, the real K_d values are in the low millimolar range (1–2 mM) (Gordon-Weeks *et al.* 1997).

Phylogenetic analysis of a large number of H^+-PPase sequences indicates that K^+-dependent and K^+-independent enzymes constitute two independently evolving subfamilies (Perez-Castineira *et al.* 2001; Belogurov *et al.* 2002b). Experimental verification of *Carboxydothermus hydrogenoformans* H^+-PPase (Ch-PPase) as a K^+-dependent enzyme, together with an assumption that K^+ dependence was lost or acquired at a specific point in H^+-PPase evolution, allows unambiguous assignment of H^+-PPase sequences to either K^+-dependent or K^+-independent subfamilies (Belogurov and Lahti 2002a). In the phylogenetic tree of membrane PPase sequences (Fig. 3), node A gives rise to branches leading to characterized K^+-dependent enzymes, signifying that the ancestor at node A was a K^+-dependent enzyme. Similarly, node B is the ancestor of K^+-independent enzymes. As any available H^+-PPase sequence is a descendant of an ancestor of either node A or node B, the K^+-dependence of H^+-PPases is readily predictable. Inspection of aligned H^+-PPase sequences reveals that only a few residues are conserved in a subfamily-specific manner. Thus, the residue corresponding to position 460 in Ch-PPase is invariably Ala in K^+-dependent enzymes and Lys in K^+-independent enzymes (the A/K site in Fig. 3). Similarly, the residue corresponding to site 463 in Ch-PPase is Ala (or Gly) in members of the K^+-dependent subfamily and Thr in K^+-independent enzymes (the G(A)/T site in Fig. 3). When these specifically conserved residues were inserted into Ch-PPase, it was found that introduction of Lys in place of Ala at the A/K site abolished enzyme K^+-dependence, whereas Thr in the G(A)/T site had no such dramatic effect. Thus, the A/K site appears to be a major determinant of K^+-dependence in H^+-PPases. Structurally, this may be explained by assuming that the NH_3^+ group of Lys occupies the space in Ch-PPase normally used by a K^+ ion. However, several unidentified residues likely contribute to the structure and function of the K^+ binding site, and thus it is not surprising that substitution of Ala into the A/K site of a K^+-independent Sc-PPase failed to confer K^+ dependence on this enzyme (Hirono *et al.* 2005).

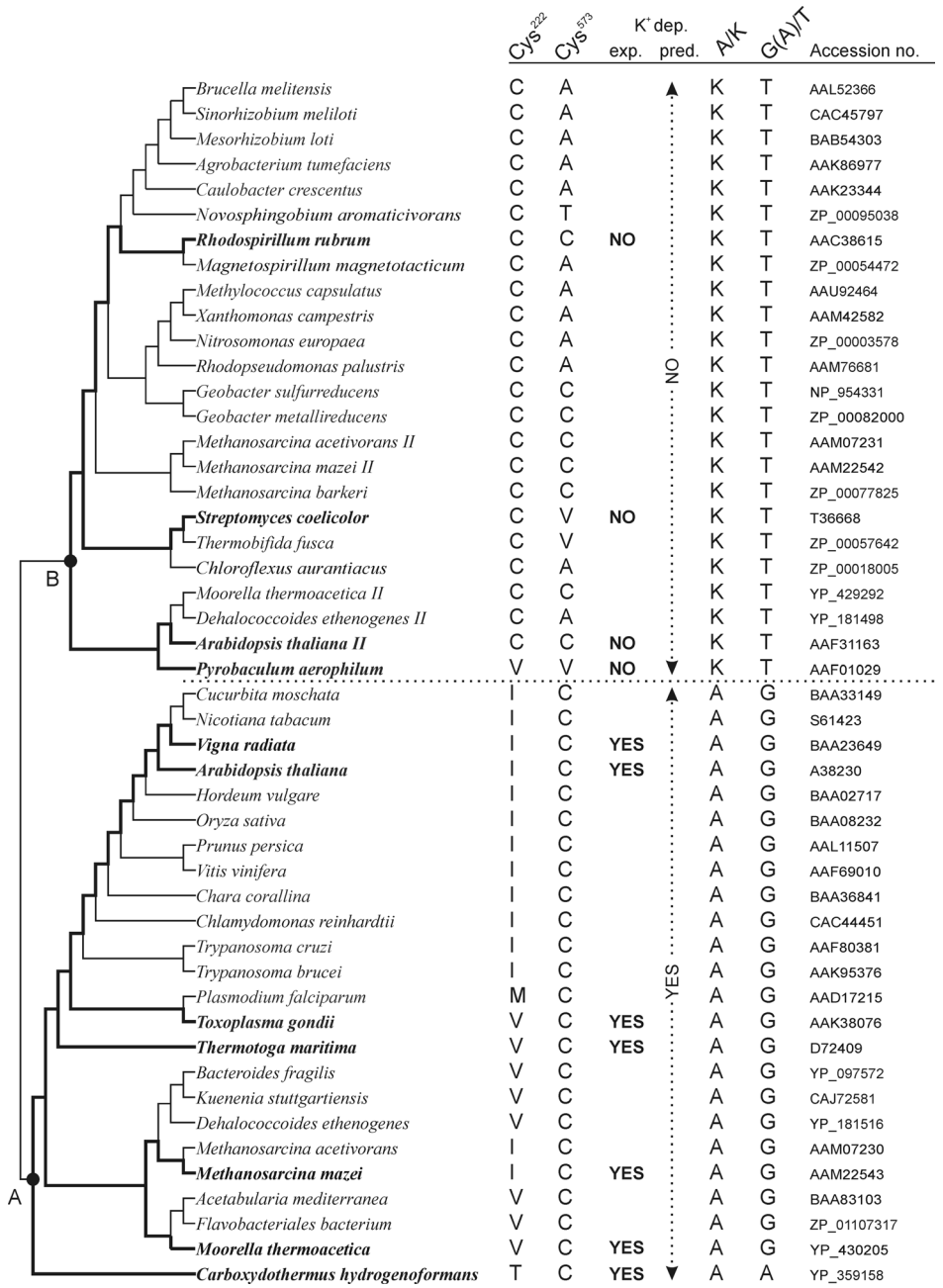

Figure 3. Two subfamilies of H^+-PPases, defined by phylogenetic analysis, Cys conservation patterns, and K^+ requirements (modified from ref. (Belogurov 2004)). The phylogenetic tree (cladogram) is arbitrarily rooted with the *C. hydrogenoformans* H^+-PPase sequence to highlight the subfamilies. Functionally characterized H^+-PPases are marked in bold and their K^+ requirements are traced back along the branches (bold lines) to nodes A and B (black circles). The columns to the right of the tree indicate residues corresponding to Cys^{222} and Cys^{573} of *R. rubrum* H^+-PPase by multiple sequence alignment, K^+ requirements of functionally characterized enzymes (K^+ dep./exp.), predicted K^+ requirements of all enzymes (K^+ dep./pred.), residues in the A/K and G(A)/T positions by multiple sequence alignment, and protein sequence accession numbers in GenBank™.

In addition to A/K and G(A)/T sites, H^+-PPases subfamilies show distinct Cys residue conservation patterns (Belogurov *et al.* 2002b). Thus, Cys at position 573 in *R. rubrum* H^+-PPase (R-PPase) is universally conserved in K^+-dependent H^+-PPases but is only sporadically present in K^+-independent enzymes (Fig. 3). Cys corresponding to position 222 is, on the other hand, conserved only in K^+-independent H^+-PPases. The cysteines are dispensable for K^+ binding or catalytic activity, but may participate in enzyme redox regulation by forming disulfides (Kim *et al.* 1995; Belogurov *et al.* 2002b). Indeed, oxidation of *S. coelicolor* H^+-PPase *in vitro* resulted in reversible and inhibitory disulfide bond between Cys^{253} (corresponding to Cys^{222} in R-PPase) and Cys^{621} of the same subunit (Mimura *et al.* 2005a). In a few cases, organisms have genes for both K^+-dependent and K^+-independent H^+-PPases. Differences in enzyme physiological roles have remained largely unexplored. Subfamily-specific intracellular localization has been reported only in plants, in which the major vacuolar H^+-PPase belongs to the K^+-dependent subfamily whereas the K^+-independent enzyme localizes to Golgi and endoplasmic reticulum membranes (Sarafian *et al.* 1992a; Mitsuda *et al.* 2001).

1.4.3 Mg^{2+} as cofactor

All H^+-PPases strictly require Mg^{2+} for activity. Detailed analysis of Mg^{2+} cofactor effects, and elucidation of the true substrate of H^+-PPase, are complicated by the fact that complexes and ions present in the reaction medium include free Mg^{2+}, free PP_i, $MgPP_i$, and Mg_2PP_i, as well as various protonated complex forms. PP_i functions as substrate only when complexed with Mg^{2+}. Some reports have suggested that $MgPP_i$ is the active substrate species (Walker and Leigh 1981; Wang *et al.* 1986; Sosa *et al.* 1992), whereas newer and more quantitative kinetic modeling studies rather suggest Mg_2PP_i as the active component (Leigh *et al.* 1992; Baykov *et al.* 1993b; Baykov *et al.* 1996a; GordonWeeks *et al.* 1996). The reported K_m values for Mg_2PP_i are in the range 1–5 μM.

In addition to functioning as a substrate component, Mg^{2+} binds directly to the enzyme, with micromolar affinity (dissociation constant 20–70 μM) (Baykov *et al.* 1993b; Baykov *et al.* 1996a; Fukuda *et al.* 2004). Mg^{2+} binding to free enzyme protects the protein against reaction with covalent inhibitors and thermal denaturation (Ordaz *et al.* 1992) and permits attainment of a conformation competent in substrate binding. Second, a low-affinity Mg^{2+} binding site (dissociation constant 0.66 mM) was proposed to exist in *R. rubrum* H^+-PPase, based on steady-state kinetic measurements (Baykov *et al.* 1996a). Therefore, 3–4 Mg^{2+} ions participate in formation of the catalytically competent enzyme–substrate complex (Baykov *et al.* 1993b; Baykov *et al.* 1996a). The Mg^{2+} binding mode is either positively cooperative (White *et al.* 1990; Fraichard *et al.* 1996) or non-cooperative (Leigh *et al.* 1992; Sosa *et al.*

1992; Baykov *et al.* 1993b; Baykov *et al.* 1996a). Mg^{2+} and K^+ ions bind to distinct sites in K^+-dependent H^+-PPases (Baykov *et al.* 1993b).

1.4.4 pH dependence

H^+-PPases are usually assayed near their pH optima (7–8), and only a few studies have directly addressed the influence of pH on catalysis. The K^+-dependent *V. radiata* enzyme has maximal activity around pH 7.0. At least four ionizable groups are essential for catalysis. Groups with pK_a values of 5.7 and 8.6 are involved in substrate binding, and groups with pK_a values of 6.1 and 9.0 are essential in the substrate-conversion step (Baykov *et al.* 1993b). The optimal functional pH values of the *S. coelicolor* and *R. rubrum* K^+-independent H^+-PPases were 7.5–8.0 and 6.5, respectively (Romero *et al.* 1991; Hirono *et al.* 2005). The latter enzyme additionally uses a basic group with a pK_a of 7.2–7.7 to bind Mg^{2+} (Baykov *et al.* 1996a).

1.4.5 Synthesis of PP_i

H^+-PPase mediates the synthesis of PP_i at a significant rate *in vitro* (Baltscheffsky *et al.* 1966; Guillory and Fisher 1972). Artificial or electron transport chain-mediated ΔpH or $\Delta\Psi$ gradients, or both, increase the synthesis rate (Strid *et al.* 1987), but the gradients are not obligatory as the synthesis rate ranges as high as 0.6% of the PP_i hydrolysis rate in non-energized vesicles (Belogurov *et al.* 2002b). PP_i synthesis activity is affected by Mg^{2+} and P_i concentrations, and is sensitive to inhibitors affecting hydrolytic activity. In comparison to ATP-synthase, the synthetic activity of H^+-PPase is activated at a lower proton-motive force and in the absence of $\Delta\Psi$, but enzyme efficiency in highly energized membranes was six-fold lower than that of ATP-synthase (Guillory and Fisher 1972; Nyren *et al.* 1986). H^+-PPase catalyzes two further measurable activities, namely P_i/PP_i phosphorous exchange (Keister and Raveed 1974) and P_i/H_2O oxygen exchange (Harvey and Keister 1981; Baykov *et al.* 1994). These activities arise from partial reversal of the overall reaction $PP_i \leftrightarrows 2P_i + (\Delta\mu_H+)$ and likely lack physiological significance. However, the exchange reactions, and the P_i/H_2O oxygen exchange in particular, may prove useful in elucidating the rates of individual reaction steps in catalysis by H^+-PPase, as has been the case in work with soluble PPases (Baykov *et al.* 1996b; Zyryanov *et al.* 2004) and ATP-synthase (Berkich *et al.* 1991).

1.4.6 Transport activity

PP_i-dependent generation of ΔpH and $\Delta\Psi$ has been demonstrated in many systems, such as bacterial membrane vesicles (Guillory and Fisher 1972; Nore *et al.* 1990), plant vacuoles (Johannes and Felle 1990; Ros *et al.* 1995), protist acidocalcisomes (Scott *et al.* 1998), and proteoliposomes containing purified H^+-PPase (Britten *et al.* 1992). ΔpH and $\Delta\Psi$ are typically monitored by assessing changes in fluorescence of acridine or Oxonol dyes, respectively.

Alternatively, patch-clamping studies using intact vacuoles (Hedrich *et al.* 1989; Davies *et al.* 1991) have demonstrated inwardly directed PP_i-dependent currents, confirming that H^+-PPase functions as an electrogenic proton pump.

Several methods have been employed to measure the number of protons transported per molecule of PP_i hydrolyzed (the coupling ratio). Schmidt and Briskin (Schmidt and Briskin 1993) calculated the coupling ratio of the *B. vulgaris* enzyme kinetically, by comparing rates of H^+-transport and PP_i-hydrolysis. The H^+-transport rate was estimated by two methods. The time course of PP_i-dependent ΔpH formation was mathematically modeled, and the initial rate of steady-state ΔpH relaxation was measured after H^+-PPase activity was abruptly terminated by EDTA addition. Both methods yielded values of unity for the coupling ratio. Similarly, Nakanishi and co-workers (Nakanishi *et al.* 2003) calculated a coupling ratio of unity for the recombinant *V. radiata* enzyme, using PP_i-dependent patch clamping current measurements. Coupling ratios can also be calculated thermodynamically by noting that the number of transported protons (n) is limited by the amount of free energy released per hydrolyzed PP_i molecule ($\Delta G'_{PPi}$) and the maximal magnitude of $\Delta\mu_H+$ ($n \leq \Delta G'_{PPi}/\Delta\mu_H{}^+$). In vacuolar membrane vesicles, H^+-PPase is capable of pumping protons against a 10,000-fold concentration gradient ($\Delta\mu_H{}^+ \approx 23$ kJ/mol)(Hedrich *et al.* 1989; Johannes and Felle 1990) or of creating a membrane potential of more than 250 mV ($\Delta\mu_H{}^+ \approx 24$ kJ/mol)(Ros *et al.* 1995). As $\Delta G'_{PPi}$ is 30–33 kJ/mol *in vitro* (at low P_i), the noted $\Delta\mu_H{}^+$ values cannot be readily obtained if the H^+/PP_i coupling ratio is greater than unity (Johannes and Felle 1990; Davies *et al.* 1993; Schmidt and Briskin 1993).

In contrast to plant enzymes, an H^+/PP_i coupling ratio of 2 has been reported in chromatophores of *R. rubrum* (Sosa and Celis 1995). This is reasonable, as the reversibility of *R. rubrum* H^+-PPase activity is well documented (Baltscheffsky *et al.* 1966; Guillory and Fisher 1972; Nyren *et al.* 1986). A coupling ratio of 2 would allow the enzyme to commence reversal at ΔpH=2, or even lower, as the concentration gradient is usually accompanied by a membrane potential. On the other hand, an enzyme with a coupling ratio of unity requires a $\Delta\mu_H+$ of double that level to reverse efficiently. Such a high gradient may be almost unachievable under experimental conditions used to activate PP_i synthesis *in vitro*, as bacterial membrane vesicles are relatively leaky. However, it remains unclear whether an H^+/PP_i coupling ratio of 2, and consequent easy reversibility, is a general property of K^+-independent H^+-PPases in photosynthetic and respiratory membranes.

Whereas the H^+-transport activity of H^+-PPases is firmly established, the proposed K^+-transport function of K^+-dependent H^+-PPases (Davies *et al.* 1992) is highly controversial. The primary evidence for K^+ transport is the

cytoplasmically directed P_i-dependent current detected by patch clamping, provided that K^+ was present inside intact vacuoles (Davies *et al.* 1992; Obermeyer *et al.* 1996). This current could be mediated by K^+-transporting H^+-PPase acting in the reverse mode. However, all attempts to detect active build-up of K^+ gradients in connection with PP_i-hydrolysis have been unsuccessful. Thus, the purified and reconstituted enzyme was unable to actively accumulate $^{42}K^+$ inside proteoliposomes (Sato *et al.* 1994). K^+ transport was similarly undetectable in vacuolar membrane vesicles multilabeled with fluorescent probes for K^+, H^+, and membrane potential (Ros *et al.* 1995). In both studies, PP_i hydrolysis was stimulated by protonophores but not by K^+ ionophores. The fact that a non-transportable NH_3^+ group introduced by A460K substitution eliminated the K^+ dependence of *C. hydrogenoformans* H^+-PPase also argues against an active K^+ transport function of K^+-dependent H^+-PPases (Belogurov and Lahti 2002a). However, it remains possible that, under specific conditions, K^+ may diffuse across the membrane via the proton conduction channel of H^+-PPase.

1.5 Expression

The first recombinant H^+-PPase was the *A. thaliana* enzyme expressed in *S. cerevisiae* (Kim *et al.* 1994). Yeast was chosen for heterologous expression as it is a vacuolate host, does not contain H^+-PPase, is amenable to molecular genetic manipulation, and had already been used to express several types of membrane proteins. The general applicability of yeast for H^+-PPase expression is now well established and successfully expressed H^+-PPases include, for example, two more plant enzymes (one from *V. radiata* (Nakanishi *et al.* 2001) and the second from *A. thaliana* (Drozdowicz *et al.* 2000)), one algal enzyme (from *Acetabularia acetabulum* (Ikeda *et al.* 2002)), two protozoan proteins (from *T. cruzi* (Hill *et al.* 2000) and *T. gondii* (Drozdowicz *et al.* 2003)), one archaeal enzyme (from *Pyrobaculum aerophilum* (Drozdowicz *et al.* 1999)), and one bacterial protein (from *T. maritima* (Perez-Castineira *et al.* 2001)). However, the yields of H^+-PPases were often low, and reported specific activities were often less than in native membranes (Kim *et al.* 1994; Drozdowicz *et al.* 2000). Technical improvements, including use of protease-deficient yeast strains, expression plasmid optimization, and employment of N-terminal signal sequences, have recently significantly increased expression levels of H^+-PPases (Nakanishi *et al.* 2003; Drake *et al.* 2004).

Yet higher expression of functional prokaryotic H^+-PPases is seen in *E. coli* (Belogurov *et al.* 2002b). The specific activity of an enzyme expressed in *E. coli* membrane vesicles was an order of magnitude higher than that in chromatophores of *R. rubrum* (Belogurov *et al.* 2002b). For high efficiency expression, the H^+-PPase gene is cloned into pET-type vectors (Novagen) under the control of the T7/*lac* promoter, and the construct is expressed in

C41(DE3) and C43(DE3) strains specifically engineered for efficient membrane protein production (Miroux and Walker 1996). H^+-PPase expression, albeit at significantly lower levels, is also evident in the more conventional strains BL21(DE3) (Novagen)(Belogurov *et al.* 2002b) and BLR(DE3)pLysS (Novagen)(Mimura *et al.* 2004). Factors important to achieve high expression include the use of rich media, long induction times (4.5–6 hours), and the use of an inducer (isopropyl-β-D-thiogalactopyranoside) concentration that only slightly inhibits cell growth (Belogurov *et al.* 2002b).

1.6 Purification

H^+-PPase has been successfully solubilized from the chromatophores of *R. rubrum* using 2% cholate (Rao and Keister 1978), 2% Triton X-100 (Nyren *et al.* 1984; Baltscheffsky and Nyrén 1986), or a 1.5% MEGA-9 0.5% cholate mix (Nyren *et al.* 1991) in the presence of 0.75 M $MgCl_2$ and 30% glycerol or ethylene glycol. Hydroxyapatite chromatography afforded good separation but homogenous H^+-PPase preparation required further purification using polyethylene fractionation and affinity chromatography (Nyren *et al.* 1991).

In comparison to enzymes from bacterial sources, H^+-PPase is more easily purified from plant vacuoles. Use of young plant tissues, such as seedling hypocotyls, is necessary because mature tissues of most plants have low levels of H^+-PPase. Pre-treatment of vacuoles with 0.3% deoxycholate removed 30% of contaminating proteins (Maeshima and Yoshida 1989). Subsequently, H^+-PPase can be solubilized using 0.4% lysophosphatidylcholine (Maeshima and Yoshida 1989; Sato *et al.* 1991), 2.5% Chaps (Britten *et al.* 1992), 2–2.5% Triton X-100 (Rea and Poole 1986; Sarafian and Poole 1989), or 1.2% *n*-octyl-β-D-glucopyranoside (Becker *et al.* 1995). Subsequent anion exchange and gel filtration chromatography steps frequently yield apparently pure H^+-PPases.

N-terminally His-tagged *T. maritima* recombinant enzyme has been purified after expression in yeast (Lopez-Marques *et al.* 2005). Purification exploited the high thermal stability of the *T. maritima* enzyme by solubilization in 1.4% *n*-dodecylmaltoside at 70°C. The membrane PPase retained solubility and activity at the elevated temperature, provided that the stabilizing ligands Mg^{2+}, K^+, and PP_i were present, whereas most yeast proteins unfolded and aggregated, and were subsequently removed by centrifugation. The heat shock alone yielded a 26-fold purification of membrane PPase and further purification using metal affinity chromatography resulted in pure, monodisperse protein. The yield of purified PPase was approximately 1.5 mg/L of yeast culture. As with all H^+-PPases purified to date, the *T. maritima* enzyme required lipid addition for attainment of maximal activity.

1.7 Functional residues

1.7.1 Covalent inhibition

H^+-PPases are inhibited by sulfhydryl-modifying reagents such as *N*-ethylmaleimide (NEM) and mersalyl (Randahl 1979; Britten *et al.* 1989; Baykov *et al.* 1993b; Baykov *et al.* 1996a). Inhibition seems to be mediated by steric effects, which arise from addition of a bulky group to the cysteine side chain. Direct participation of cysteines in catalysis is unlikely because substitution of Cys residues in H^+-PPases of *A. thaliana* (Kim *et al.* 1995) and *S. coelicolor* (Mimura *et al.* 2004) showed only a modest inhibitory effect (<50%) on hydrolytic and H^+-transport activities. In addition, the enzyme from the hyperthermophilic bacterium *P. aerophilum* lacks cysteine residues (Drozdowicz *et al.* 1999). [^{14}C]NEM labeling (Zhen *et al.* 1994b) and site-directed mutagenesis (Kim *et al.* 1995) of *A. thaliana* H^+-PPase indicated that Cys^{634}, a residue conserved in all K^+-dependent H^+-PPases, was the target for modification and inhibition by sulfhydryl reagents. The corresponding cytoplasmically oriented cysteine was also reactive in pumpkin H^+-PPase (Maruyama *et al.* 1998). In contrast, the K^+-independent *R. rubrum* enzyme was inhibited by NEM and mersalyl in a biphasic manner, indicating at least two reactive cysteines (Baykov *et al.* 1996a). In the rapid phase (complete in a few seconds), Cys^{222}, specific to the K^+-independent enzyme subfamily, reacted, resulting in a ~20% decrease in catalytic activity (Belogurov *et al.* 2002b). Complete inactivation occurred on a slower time scale (over minutes), and probably involved modification of both Cys^{185} and Cys^{573}. Notably, Cys^{573} aligns with Cys^{634} of the *A. thaliana* enzyme. Mg^{2+} partially protected against sulfhydryl reagent inhibition, free PP_i enhanced inhibition, and a combination of Mg^{2+} and PP_i provided full protection (Randahl 1979; Britten *et al.* 1989; Baykov *et al.* 1993b; Zhen *et al.* 1994b; Baykov *et al.* 1996a; Maruyama *et al.* 1998).

Covalent modification of histidine residues using diethylpyrocarbonate or 4-bromophenacyl bromide also inhibited H^+-PPase activities in a ligand-dependent manner (Hsiao *et al.* 2002; Schultz and Baltscheffsky 2004). H^+-PPases share only one fully conserved His, and even this residue, and all other His residues, can be functionally substituted in *R. rubrum* and *V. radiata* enzymes (Hsiao *et al.* 2004; Schultz and Baltscheffsky 2004). Even though the conserved His^{716} (*V. radiata* numbering) is probably not a catalytic residue, substitution of this His with Ala rendered the variant enzyme less susceptible to inhibition, suggesting that His^{716} is the primary target for His-specific reagents (Hsiao *et al.* 2004).

H^+-PPase is additionally inhibited by compounds that target Lys, Arg, or Asp/Glu/C-terminal residues, but is not inhibited by compounds specific for

Tyr (GordonWeeks *et al.* 1996; Yang *et al.* 2000; Schultz and Baltscheffsky 2004). Again, substrate binding protected against inhibition. Fluorescein 5′-isothiocyanate, a Lys-specific reagent, mainly targeted the conserved Lys^{469} in *R. rubrum* H^+-PPase (Schultz and Baltscheffsky 2004). This residue also has functional significance, as substitution with Ala or Arg either inactivated the enzyme completely or eliminated 93% of wild-type activity, respectively (Schultz and Baltscheffsky 2003). All 15 Arg residues were progressively substituted with Ala in *V. radiata* H^+-PPase (Hsiao *et al.* 2007). Substitution of the near-conserved Arg^{242} resulted in low activity (7% of wild-type) that was only slightly inhibited by the Arg-modifying reagents phenylglyoxal and 3-butanedione. Therefore, Arg^{242} may represent the primary target of these compounds. Notably, substitution of conserved Arg^{170} and Arg^{272} residues decreased enzymatic activity by only 50%, suggesting that the reason for strict residue conservation is more complex than direct roles for these residues in catalysis. *N,N'*-dicyclohexylcarbodiimide (DCCD), a carboxyl-specific reagent, appeared to modify different non-conservative residues in various K^+-dependent plant H^+-PPases. Thus, E305Q and D504N substitutions markedly decreased the sensitivity of *A. thaliana* enzyme to DCCD (Zhen *et al.* 1997), whereas peptide mapping using fluorescent and radioactive DCCD analogues indicated labeling of Glu^{749} near the C-terminal end of pumpkin H^+-PPase (Maruyama *et al.* 1998) and Asp^{283} in the third cytoplasmic loop of the *V. radiata* enzyme (Yang *et al.* 1999). The residue corresponding to Asp^{283} of the *A. thaliana* enzyme appeared to react with DCCD also in the K^+-independent *R. rubrum* H^+-PPase (Schultz and Baltscheffsky 2004). If DCCD labeling targets different residues in various H^+-PPases, it seems unlikely that the compound will be useful to delineate carboxyl groups potentially participating in proton conduction.

1.7.2 Loops

Most of the 60 conserved residues of the H^+-PPase protein family cluster to the cytoplasmic loops *e*, *k,* and *o* (light blue residues in Fig. 4), suggesting that these three loops form a major part of the active site for PP_i hydrolysis. Nakanishi and coworkers (Nakanishi *et al.* 2001) first tested this hypothesis, using K^+-dependent *V. radiata* H^+-PPase, by substituting several charged residues (Asp^{253}, Lys^{261}, Glu^{263}, Asp^{279}, Asp^{283}, Asp^{287}, Asp^{723}, Asp^{727}, and Asp^{731}) in three highly-conserved motifs of cytoplasmic loops *e* and *o*. The corresponding residues in Sc-PPase are indicated by asterisks (*) in Fig. 4. Consistent with functional importance, substitutions by Ala, or more similar residues (*i.e.,* Asp→Glu, Glu→Asp and Lys→Arg), yielded inactive enzymes, except for the K261R and E263D variants, which retained 30% and 60% of wild-type hydrolytic activity, respectively. Substrate binding protected wild-type enzyme against trypsin digestion, but the effect was diminished in several variants. K261A, K261R, and E263A variant enzymes were particularly

susceptible to digestion, suggesting involvement of the substituted residues in substrate binding. Substitution of Asp^{217} or Glu^{231} (corresponding to residues D248 and E262, marked by # symbols in Fig. 4) inactivated *R. rubrum* H^+-PPase, indicating that cytoplasmic loop *e* was also important for function of K^+-independent enzymes (Schultz and Baltscheffsky 2003). With the same enzyme, two further residues, Asp^{428} and Lys^{469} (corresponding to E469 and K511 in Sc-PPase), located at the predicted interface between the membrane and cytoplasmic loop *k*, were found to be essential (Schultz and Baltscheffsky 2003). The functional importance of the C-terminal polypeptide end was verified in *V. radiata* H^+-PPase (Lin *et al.* 2005). A variant lacking the last five residues (ΔC5) showed less than 20% of wild-type activity. Interestingly, an enzyme truncated by 10 residues was more active (75% of wild-type), whereas longer deletions (ΔC14, ΔC20, and ΔC25) completely abolished activity. Thus, the C-terminus appears to contribute to H^+-PPase functional conformation, perhaps by placing the nearby conserved sequence motif of cytoplasmic loop *o* in the correct position.

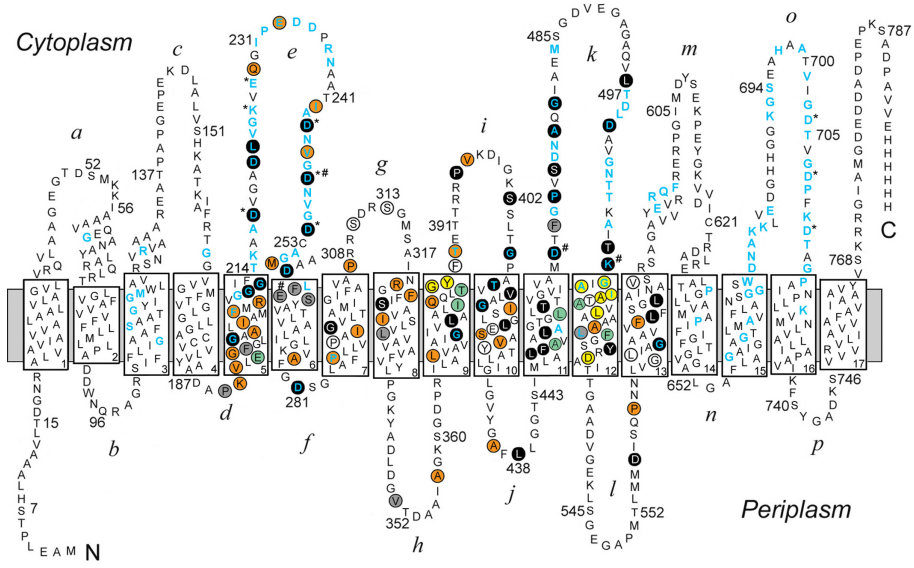

Figure 4. Mutagenesis of *S. coelicolor* H^+-PPase (Sc-PPase). The conserved residues in the H^+-PPase family are depicted by light blue letters in the topological model of Sc-PPase (Mimura *et al.* 2004). The circles indicate residues substituted in Sc-PPase (Hirono *et al.* 2007; Hirono *et al.* 2007). The effects of substitutions on the hydrolytic and H^+-transport activities of Sc-PPase variants were classified into six categories, as in the original reports, and are indicated by different circle fill colors: black, no activity; grey, low hydrolytic activity (10–25% of wild-type) but no H^+-transport activity; orange, H^+-transport activity decreased more than did hydrolytic activity resulting in decreased coupling ratios (10–70% of wild-type); light green, decreased hydrolytic activity but no change in coupling ratio; yellow, increased coupling ratio (>120% of wild-type); white, no apparent effect. Residues corresponding to substituted residues in *V. radiata* and *R. rubrum* H^+-PPase are indicated by * and # symbols, respectively. The Figure is modified from ref. (Mimura *et al.* 2004).

Hirono and coworkers prepared two libraries of variant Sc-PPases by subjecting the second (Hirono *et al.* 2007) and third quarters (Hirono *et al.* 2007) of the relevant gene to random mutagenesis. The libraries were expressed in *E. coli* and 3,000 mutants were assayed for H^+-PPase expression, PP_i hydrolysis, and H^+-transport. Mutants characterized by low hydrolytic activity or ineffective energy coupling were analyzed in more detail and DNA sequencing was performed. Sixty-eight single substitutions at 66 residue positions were identified. The random mutagenesis was complemented by specifically substituting 47 semi-conserved/conserved (particularly Gly, Ser, and Pro) or charged residues located in or close to transmembrane segments. Overall, the functional significances of 25% of 404 residues in the Sc-PPase middle sector were examined. The analysis identified 41 residues indispensable for detectable activity (indicated by black circles in Fig. 4). Most of these functionally essential residues are conserved in the H^+-PPase family and cluster to the cytoplasmic loops *e* and *k*. Interestingly, the poorly conserved loop *i* also appeared functionally important, whereas loop *g* tolerated substitutions. These results, together with an earlier demonstration of loop *o* functionality (Nakanishi *et al.* 2001), suggest that several loops pack tightly together to form a catalytically competent structure in the H^+-PPase cytoplasmic segment. The work further identified three periplasmic substitutions (D281G, L438P, and D556G) completely inactivating the enzyme. Direct participation by these residues in catalysis is unlikely. Probably, significant structural alterations provoked a long-range conformational perturbation of H^+-PPase.

1.7.3 Residues affecting H^+ translocation

Significant effort has been invested in elucidating the residues and structural elements contributing to the coupling of PP_i hydrolysis activity to proton transport. Substitution of a semi-conserved Glu^{427} in the *A. thaliana* enzyme had a pronounced effect on H^+ transport activity resulting in a decreased coupling ratio (H^+ transport rate divided by PP_i hydrolysis rate) in the E427Q variant, whereas the coupling ratio increased in the E427D variant (Zhen *et al.* 1997). K461A substitution in the same cytoplasmic loop *i* (or possibly in the adjoining transmembrane segment) also yielded a low coupling variant, whereas inversion of charges in the E427K/K461E double variant restored full coupling (Zancani *et al.* 2007). Thus, Glu^{427} and Lys^{461} likely play indirect roles in H^+-translocation. Possibly, a salt bridge between the residues holds the enzyme in a conformation competent for H^+-transport. Notably, substitution of the corresponding Glu residue in the *R. rubrum* enzyme also inhibited H^+ transport, albeit to a lesser extent (Schultz and Baltscheffsky 2003). Substitution of the first Gly (corresponding to Gly^{209} in Sc-PPase) in the triple Gly motif at the cytoplasm–membrane interface of cytoplasmic loop *e* had a more detrimental effect on H^+-transport activity than on hydrolytic activity. A similar but smaller effect was achieved by a nearby R176K substitution (Arg^{207}

in Fig. 4). The data may mean that the triple Gly motif provides important flexibility in local protein structure promoting efficient coupling of hydrolytic and transport activities.

Large-scale mutagenesis of Sc-PPase (Hirono *et al.* 2007; Hirono *et al.* 2007) revealed that several substitutions in the transmembrane (TM) helices caused functional defects of variable severity (Fig. 4). The most disruptive substitutions involved many Gly and non-polar residues that generally stabilize membrane protein structures by facilitating interactions between TM helices (Bowie 2005). Many variants that retained partial hydrolytic activity had relatively low H^+-transport rates, suggesting decreased coupling efficiencies (grey and orange circles in Fig. 4). A particularly high proportion of such substitutions mapped to the two sides of TM helix 5, which may thus interact with other helices in the TM helix bundle anchoring the functionally important cytoplasmic loop *e* in the correct position. Alanine scanning mutagenesis of TM helix 5 in the *V. radiata* H^+-PPase also yielded some low coupling variants (Van *et al.* 2005). Furthermore, G211A and G210A variant Sc-PPases had only low activities, confirming the functional significance of the triple Gly motif at the cytoplasmic end of TM helix 5. A curious set of substitutions, located in the cytoplasmic segments of TM helices 9 and 12, increased apparent coupling ratios by 25–100% (yellow circles in Fig. 4). In principle, the observation may indicate that variant enzymes transport more protons per PP_i hydrolyzed than does the wild-type enzyme.

2 AIMS OF THE STUDY

It is well-known that several types of ATP-dependent primary H^+-transporters have closely related homologues transporting Na^+ ions instead of H^+ (Mulkidjanian *et al.* 2008). The importance of maintaining low internal Na^+ concentrations via active Na^+ transport and exchange reactions is further emphasized by the existence of Na^+ pumps energized by decarboxylation of dicarboxylates, oxidation of NADH, and methyl transfer (Mulkidjanian *et al.* 2008). In addition, some bacteria use a membrane Na^+ gradient instead of an H^+ gradient as a source of energy for cellular processes. PP_i-dependent H^+-transport has long been known (Moyle *et al.* 1972). In this study, we exploited the exponential growth of microbial sequence information and decided, i) to ascertain whether some organisms employed variant membrane-bound PPases to transport Na^+ ions, and, ii) when Na^+-transporting PPases were indeed found, to functionally characterize such enzymes, with particular attention to ligand-binding properties, and, iii) as a separate project, to determine the functional significance of charged universally conserved residues in the cytoplasmic segment of a H^+-transporting PPase.

3 METHODS

3.1 Sample preparation

Mutagenesis of membrane PPase genes was performed using overlapping or inverse PCR (Stemmer and Morris 1992). The sequenced genes were assembled in pET22b(+) or pET36b(+) vectors (Novagen) and expressed in *E. coli* C41(DE3) and C43(DE3) strains (Belogurov *et al.* 2002b). Cells were disrupted either by sonication or by passage through a French pressure chamber. Cell lysates were subjected to differential centrifugation to isolate recombinant proteins as components of inner membrane vesicles (IMVs). To estimate molecular masses, proteins were fractionated by SDS-PAGE (Laemmli 1970) and membrane PPases were visualized by immunodetection or staining with Coomassie Brilliant Blue.

3.2 Assays of membrane PPase activities

Because *E. coli* lacks endogenous membrane PPase and soluble *E. coli* PPase is efficiently washed away during IMV isolation, the IMVs could be used directly to measure hydrolytic activities of membrane PPases. The concentrations of reaction buffer components (buffer, H^+, EGTA, Mg^{2+}, Na^+, K^+, and PP_i) were chosen after considering the dissociation constants of the Mg^{2+}, Na^+, K^+, and H^+ complexes of PP_i (Baykov *et al.* 1993b), and reactions were commenced by addition of IMV suspensions. Liberation of inorganic phosphate was continuously recorded over approximately 3 min at controlled temperatures (25–80°C) using a flow-through phosphate analyzer (Baykov and Avaeva 1981). Each reaction rate was calculated from the initial slope of the recorded curve, and was typically normalized to total protein concentration as determined by the Bradford assay (Bradford 1976). In the case of *T. maritima* membrane PPase (study II), specific activity determinations employed PPase protein concentrations estimated by densitometry of Coomassie-stained SDS-PAGE gels. Reagents with low levels of contaminating Na^+ and K^+ were utilized. When PPase activity was assayed in the presence of Na^+ or K^+ at concentrations below 0.2 mM, ion concentration was determined by atomic absorption spectrometry. To determine the susceptibility of different PPase–ligand complexes to inactivation by the SH reagent mersalyl and trypsin, IMV and ligand concentrations were adjusted in 0.15–1 mL volumes and inactivators were added. Aliquots were withdrawn at various timepoints to measure residual PPase activities, as described above.

PP_i-energized H^+ transport into membrane vesicles was assayed by continuously measuring fluorescence quenching of the pH-sensitive probe acridine orange (Rosen 1986). PP_i-dependent Na^+ transport into membrane vesicles was monitored by following accumulation of $^{22}Na^+$ inside vesicles. Aliquots of reaction mixtures were withdrawn at appropriate times and passed

through Dowex 50 ion-exchange columns. The eluates contained IMVs and $^{22}Na^+$ trapped therein, whereas all external $^{22}Na^+$ remained bound to the column. The amounts of $^{22}Na^+$ in the samples were determined by liquid scintillation counting. Generation of membrane potential was detected as a red shift in the absorbance maximum of Oxonol VI dye (Waggoner 1979).

3.3 Sequence and data analysis

Membrane PPase gene sequences were downloaded from GenBank™. Multiple sequence alignments and phylogenetic analysis were performed using ClustalX version 1.8 (Thompson *et al.* 1997) and MrBayes version 3 (Ronquist and Huelsenbeck 2003), respectively. Enzyme kinetic modeling was achieved by fitting PP_i hydrolysis rates to appropriate rate equations, employing the SCIENTIST program (MicroMath). The reported kinetic schemes are minimal in the sense that elimination of any species makes fits much poorer in terms of the sums of squares of residuals, whereas addition of other intermediate species do not significantly improve the schemes.

4 RESULTS AND DISCUSSION

4.1 Discovery of Na^+-transporting PPases (studies II and III)

4.1.1 Na^+-dependent membrane PPases

We initially found that the membrane PPase of the marine bacterium *T. maritima* (Tm-PPase), assayed in *E. coli* IMVs, absolutely required Na^+ for activity. The detergent-solubilized, purified recombinant enzyme and the native enzyme in membrane vesicles of *T. maritima* similarly depended on Na^+, indicating that the Na^+ requirement was not an artifact of heterologous expression in *E. coli*. Na^+ alone activated Tm-PPase, but additional binding of K^+ further increased the maximal enzymatic activity and decreased the Na^+ concentration required for activation. In contrast, K^+ alone did not act as an activator. The ion requirement of Tm-PPase is thus distinct from those of ordinary K^+-dependent H^+-transporting PPases, which are fully activated by K^+ alone and may employ Na^+ in place of K^+ as an alternative activator. However, the similarity of Tm-PPase to H^+-PPases is indicated by common functional properties such as hypersensitivity to AMDP inhibition, requirement of Mg^{2+} for activity, and low sensitivity to inhibition by fluoride.

The absolute requirement of Tm-PPase for Na^+ raised the possibility that the enzyme transported Na^+ ions rather than H^+. However, direct experimental verification of this possibility was hampered by the low activity of hyperthermophilic Tm-PPase at temperatures (<30°C) required to maintain sufficient sealing of the vesicles used in transport assays. We therefore

searched for Na^+-dependent membrane PPases in less thermophilic organisms. Because full functional redundancy is extremely rare in prokaryotic genomes, we focused our efforts on the thermophilic acetogenic eubacterium *Moorella thermoacetica* and the mesophilic methanogenic archaeon *Methanosarcina mazei*; these organisms both possess genes for two phylogenetically distinct membrane PPases. We expressed the genes for the predicted K^+-dependent enzymes in *E. coli* and found that both proteins absolutely required Na^+ for activity and were maximally active in the presence of both Na^+ and K^+, as with Tm-PPase. Thus, Na^+ dependence is not just a curiosity restricted to Tm-PPase but rather appears to be widespread among membrane PPases.

4.1.2 Transport specificity of Na^+-dependent membrane PPases

H^+-transporting PPases expressed in *E. coli* mediate PP_i-dependent acidification of the membrane vesicle interior, conveniently assayed by quenching of acridine orange fluorescence (Belogurov and Lahti 2002a; Belogurov *et al.* 2002b). Importantly, we did not observe such quenching when Na^+-dependent membrane PPase of *M. mazei* (Mm-PPase) was assayed at pH 7.2 (Fig. 5) or at pH values of 5.5 or 9. Under similar conditions, vesicles containing the H^+-PPase of *R. rubrum* (R-PPase) displayed a strong H^+ transport signal. The lack of H^+ transport by Mm-PPase was not attributable to vesicle leakage, because generation of an H^+ gradient was evident upon addition of lactate, which becomes oxidized by the coupled action of an endogenous *E. coli* membrane enzyme D-lactate dehydrogenase and the electron transport chain (Matsushita and Kaback 1986). We thus concluded that Mm-PPase did not translocate protons across the IMV membrane.

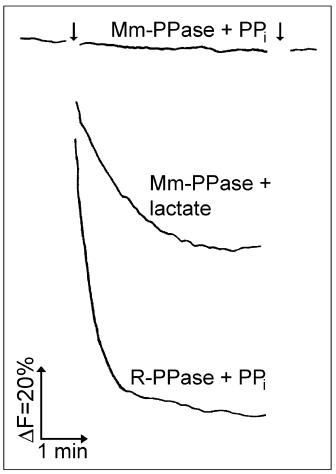

Figure 5 (study III). H^+ translocation into IMVs containing R-PPase or Mm-PPase at 25°C. The left arrow indicates the addition of PP_i or lactate, and the right arrow indicates the addition of NH_4Cl, to dissipate the H^+ concentration gradient.

To directly test the hypothesis that Na^+-dependent PPases are Na^+ transporters, we added $^{22}Na^+$ to the assay medium and separated IMVs, at various timepoints, from non-transported isotope, using ion exchange chromatography. PP_i addition indeed triggered a time-dependent accumulation of $^{22}Na^+$ inside vesicles (Fig. 6). Importantly, we did not observe Na^+ transport in authentic *E. coli* IMVs, which lack membrane PPases, or in IMVs bearing H^+-transporting R-PPase. Monensin, which allows free diffusion of Na^+ across membranes, completely prevented $^{22}Na^+$ accumulation by Mm-PPase-containing IMVs. In contrast, addition of carbonyl cyanide *m*-chlorophenylhydrazone (CCCP), a protonophore dissipator of H^+ concentration gradients, did not prevent PP_i-driven $^{22}Na^+$ uptake. Thus, rather than generating a transient H^+ gradient that can be exchanged for Na^+, Mm-PPase directly transports Na^+ across the membrane. The maximal amount of $^{22}Na^+$ accumulated in Mm-PPase-containing IMVs increased nearly tenfold when the assay temperature was increased from 0 to 25°C (Figs. 6 and 7) but remained similar when the external Na^+ concentration varied between 0.5–2 mM. Thus, both hydrolytic and pumping activities were stimulated by increases in temperature but were independent of Na^+ concentrations in the range tested. In addition, loaded $^{22}Na^+$ diffused slowly out of vesicles after Mm-PPase action was shut down by substrate depletion. These observations collectively indicate that Mm-PPase builds an Na^+ concentration gradient across IMVs, with the higher concentration inside, rather than merely permitting ion equilibration across the membrane.

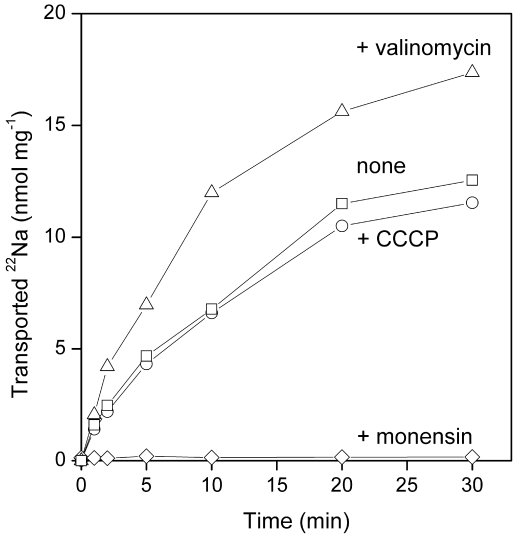

Figure 6 (study III). PP_i-energized accumulation of $^{22}Na^+$ by Mm-PPase-containing IMVs at 0°C. Each reaction was commenced by adding PP_i to a reaction mixture containing IMVs and monensin (10 μM), CCCP (20 μM), or valinomycin (2 μM), as indicated.

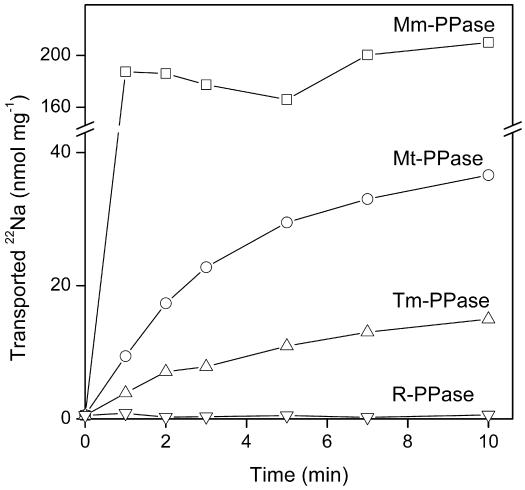

Figure 7 (study III). PP_i-energized accumulation of $^{22}Na^+$ by IMVs containing Mm-PPase, Mt-PPase, Tm-PPase, or R-PPase, at 25°C.

Further characterization of Na^+ transport activity indicated that valinomycin, which allows free diffusion of K^+ across membranes, thus dissipating any membrane potential, increased both the initial rate of $^{22}Na^+$ transport and the final level of $^{22}Na^+$ accumulation (Fig. 6). Na^+ transport additionally resulted in an absorbance maximum red shift (from 595 to 605 nm) of the optical membrane potential probe Oxonol VI, indicating formation of a positive inside potential. The red shift reverted when membrane potential was dissipated by addition of valinomycin. The evidence thus suggests that Mm-PPase is an electrogenic Na^+ transporter.

Because K^+ increases the activity of Na^+-dependent membrane PPases, we examined the possible transport of K^+ into or out of IMVs. As K^+ radioisotopes are very unstable ($t_{1/2}$ <23 h), we replaced K^+ ions of the transport assay medium by longer-lived $^{86}Rb^+$ ions ($t_{1/2}$=18.7 days) that similarly activate Mm-PPase. Addition of PP_i did not induce changes in the equilibrium concentration of $^{86}Rb^+$ inside IMVs in response to Na^+ accumulation, which, however, was also seen in Rb^+- and K^+-free media. The enzyme is thus unlikely to transport Rb^+ or its analog, K^+, either together with or in exchange for Na^+. The enzyme also appears to show a strong preference for Na^+ over H^+ as a transport substrate. Whereas H^+ could replace Na^+ as the coupling ion in Na^+,K^+-ATPase (Polvani and Blostein 1988) and Na^+-translocating F_1F_0-ATPase (Laubinger and Dimroth 1989), under low Na^+ or high H^+ concentrations, we neither observed H^+-translocation by Mm-PPase nor detected any relaxation in hydrolytic activity Na^+ dependence at any tested pH (pH 5.5–9).

After the Na^+ transport assay was optimized using mesophilic Mm-PPase, it became possible to assay transport specificities of the thermophilic Na^+-

dependent membrane PPases. Both *M. thermoacetica* PPase (Mt-PPase) and Tm-PPase catalyzed significant PP_i-driven $^{22}Na^+$ transport into *E. coli* IMVs (Fig. 7). In comparison to Mm-PPase, the transport rate was lower because the assay temperature (25°C) was far below that optimal for enzyme activity. Thus, Na^+-dependent membrane PPases generally appear to function as primary Na^+ transporters (Na^+-PPases).

4.1.3 Subfamily of Na^+-transporting PPases

The discovery of Na^+-transporting PPases explains the puzzling presence of two membrane PPase genes in several prokaryotic species. Significantly, the Na^+-PPase and H^+-PPase genes are adjacent on the chromosome of *M. mazei*, suggesting that this gene cluster may be the footprint of an ancient gene duplication preceding the split between Na^+- and H^+-transporting PPases. The duplication probably involved a K^+-dependent enzyme because Na^+-PPases are more closely related to K^+-dependent H^+-PPases than to other PPases. Thus, both types of membrane PPases contain Ala in the K^+-dependence signature sequence and accordingly display maximal activity in the presence of millimolar levels of K^+. A phylogenetic analysis of membrane PPase sequences indicates that both the K^+-independent and K^+-dependent PPase groups are monophyletic (Fig. 3). Na^+-PPases of *M. mazei*, *M. thermoacetica,* and *T. maritima* cluster with K^+-dependent H^+-PPases but do not form a monophyletic group because node A also gives rise to branches leading to the H^+-PPase of *C. hydrogenoformans* and the plant H^+-PPases. It remains to be determined whether the lack of a distinct split between the Na^+- and H^+-PPases is because of limitations in phylogenetic analysis, resulting in poor resolution near node A, or because the nature of the ions transported has changed several times during the evolution of membrane PPases.

The identification of Na^+-PPases in three evolutionarily and ecologically distant species suggests that many microbes utilize Na^+-transporting PPases. The role of Na^+-PPases in different hosts is speculative at this stage of research, but several possibilities may be suggested. Thus, the thermophilic marine bacterium, *T. maritima*, which utilizes Na^+ as the primary bioenergetic coupling ion (Dimroth and Cook 2004; Mulkidjanian *et al.* 2008), may employ Na^+-PPase to harness the energy from biosynthetic waste (PP_i) in the form of an Na^+ gradient energizing the Na^+-coupled ATP-synthase. Organisms employing H^+-coupled ATP-synthases, such as *M. mazei* and *M. thermoacetica* (Drake and Daniel 2004; Pisa *et al.* 2007), or life forms that do not depend on ion gradients to synthesize ATP, could utilize Na^+-PPase to replace or work in parallel with the Na^+/H^+ antiporter and primary Na^+ pumps to maintain low, non-toxic internal Na^+ concentrations. The fact that *M. mazei* and *M. thermoacetica* also possess genes encoding H^+-PPases suggests that these organisms may choose, depending on prevailing physiological requirements,

whether to invest the free energy of PP_i hydrolysis to transport either H^+ or Na^+ across the membrane. For example, *M. mazei* growing on methanol to mid-log phase expressed only H^+-PPase (Baumer *et al.* 2002).

4.2 Ligand binding in Na^+-transporting PPases (studies II, III, and IV)

4.2.1 Scope

Preliminary characterization of the activities of Na^+-PPases indicated absolute requirements for Mg^{2+} and Na^+, and a further role for K^+ as an auxiliary modulator. In addition to binding sites for these three ligands, each enzyme has, of course, a binding site for substrate PP_i. To investigate properties of individual ligand binding sites and interactions between these sites, we determined the steady-state rates of PP_i hydrolysis by Na^+-PPase over wide ranges of Mg^{2+}, PP_i, Na^+, and K^+ concentrations, and assessed the protection afforded by ligand binding against inactivation by the SH reagent mersalyl and protease trypsin. Thus, we defined the stoichiometry and stability of the catalytically active enzyme-substrate complex, and gathered information on the roles of different ligands in facilitating attainment of the catalytically active conformation.

4.2.2 Mg^{2+} binding sites

At fixed free Mg^{2+} concentrations (0.05–20 mM), the dependence of Mm-PPase on substrate (Mg_2PP_i) concentration obeyed the Michaelis-Menten equation, and the parameters k_h^{app} and K_m^{app} are shown in Fig. 8. The shapes of the k_h^{app} and K_m^{app} profiles measured in the presence or absence of K^+ were similar. The value of k_h^{app} increased steeply with increasing Mg^{2+} concentration, whereas K_m^{app} was almost Mg^{2+}-independent. Computational kinetic modeling of the rate data indicated a plausible scheme involving the binding of two activating Mg^{2+} ions both to the free enzyme and the enzyme-substrate complex (Scheme 1 and Table 2). To account for the small decline in k_h^{app} seen at high Mg^{2+} concentrations, a third, inhibitory Mg^{2+} binding site, yielding an inactive EMg_3S complex, was included in Scheme 1. Activating Mg^{2+} ions bind to the enzyme in a highly cooperative manner, thus the two monomagnesium species shown in brackets (EMg and EMgS) are stoichiometrically insignificant.

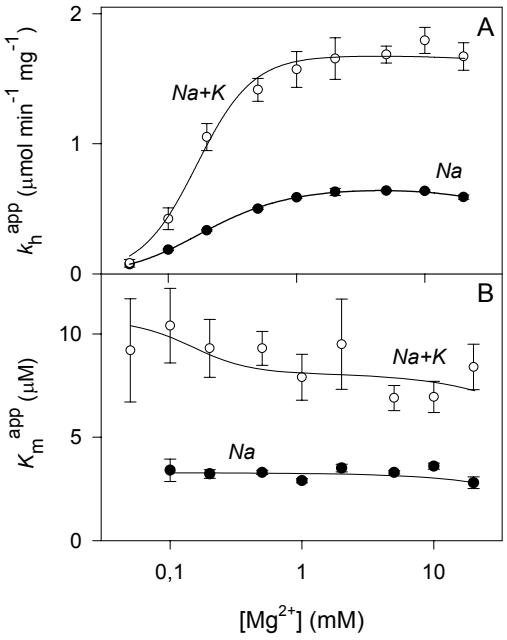

Figure 8 (study IV). Dependence of k_h^{app} (A) and K_m^{app} (for Mg_2PP_i) (B) of Mm-PPase on free Mg^{2+} concentration. Measurements were performed in the presence of 100 mM Na^+ (●), or 10 mM Na^+ and 50 mM K^+ (○), at 25°C.

Scheme 1 (study IV). Mg^{2+} and substrate (S = Mg_2PP_i) binding to Mm-PPase. The parameter values are listed in Table 2.

$$\begin{array}{ccccccc} & & K_{M1} & & K_{M2} & & \\ E & & \leftrightarrows & [EMg] & \leftrightarrows & EMg_2 & \\ & & & & & \downuparrows K_m & \\ & & K_{A1} & & K_{A2} & & K_i \\ ES & & \leftrightarrows & [EMgS] & \leftrightarrows & EMg_2S & \leftrightarrows & EMg_3S \\ & & & & & \downarrow k_h & \end{array}$$

[a] Species shown in square brackets are stoichiometrically insignificant.

Table 2 (study IV). Kinetic parameters for Mg^{2+} activation

Parameter	value	
	Na^+-activated enzyme	$Na^+ + K^+$-activated enzyme
k_h, μmol·min^{-1}·mg^{-1}	0.70 ± 0.02	1.68 ± 0.09
$K_{A1}K_{A2}$ (mM^2)	0.056 ± 0.004	0.022 ± 0.003
$K_{M1}K_{M2}$ (mM^2)	0.056 ± 0.003	0.028 ± 0.003
K_i (mM)	120 ± 30	> 200
K_m (μM)	3.3 ± 0.1	8.1 ± 0.6

4.2.3 Na^+ and K^+ binding sites

At saturating substrate and Mg^{2+} concentrations, Mm-PPase activity increased hyperbolically with increasing Na^+ concentrations to attain a plateau value (Fig. 9A). Increasing K^+ concentration progressively shifted the Na^+ dose-response curve to lower concentrations (*i.e.,* to the left) and increased maximum activity. In the presence of Na^+, activity increased with increasing K^+ concentrations (Fig. 9B). We used a simple binding scheme involving two alkali cation binding sites on the enzyme to fit the data. According to Scheme 2, the enzyme operates via two parallel routes: one is used by the K^+-free enzyme and the other by the K^+-bound enzyme. Both the high-affinity binding site that is specific for Na^+ and the low-affinity binding site that binds Na^+ and K^+ with similar affinities, must be occupied before catalysis proceeds. The high-affinity Na^+-specific site may represent the acceptor site for transported Na^+, and could therefore correspond to the H^+ acceptor site in H^+-PPases. The lower-affinity site is probably the counterpart of the cytoplasmically oriented K^+ binding site in K^+-dependent H^+-PPases (Davies *et al.* 1991). This site likely has a regulatory or structural role in Na^+- and H^+-translocating PPases. When K^+ replaced Na^+ in this site, the catalytic activity of the enzyme-substrate complex increased 2-fold and the affinity of the Na^+-specific site 10-fold (K_{Na1} vs. $K_{Na(K)}$). Likewise, Na^+ in the specific site increased the affinity of Mm-PPase for K^+ 10-fold (K_K vs. $K_K K_{Na1(K)}/K_{Na1}$).

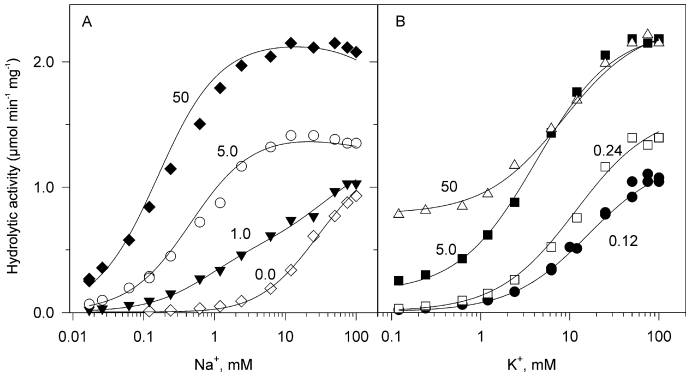

Figure 9 (study III). Dependence of the PP_i hydrolysis rate of Mm-PPase IMVs on Na^+ and K^+ at 40°C. Numbers on the curves show fixed K^+ (A) or Na^+ (B) concentrations in mM.

Scheme 2 (study III). Na^+ and K^+ activation of Mm-PPase. The numerical values for the kinetic constants are indicated in parentheses.

$$\begin{array}{lcl} & K_{Na1(K)}\ (0.1\ mM) & \quad V_1\ (2.3\ \mu mol\ min^{-1}\ mg^{-1}) \\ EK & \leftrightarrows \quad EKNa & \rightarrow \end{array}$$

$$\downarrow\uparrow K_K\ (31\ mM)$$

$$\begin{array}{lcccl} & K_{Na1}\ (1.0\ mM) & & K_{Na2}\ (30\ mM) & \quad V_2\ (1.3\ \mu mol\ min^{-1}\ mg^{-1}) \\ E & \leftrightarrows \quad ENa & \leftrightarrows & ENa_2 & \rightarrow \end{array}$$

The kinetic model of Tm-PPase activation by Na^+ and K^+ also involves parallel routes for K^+-free and K^+-bound enzymes. Tm-PPase, as with Mm-PPase, has a single binding site for activating K^+ ion, but Na^+ bound to Tm-PPase in a more complex manner. The number of essential Na^+ ions in the K^+-dependent route is increased by one ($EKNa_2$ and ENa_2 are the active species) and the enzyme additionally bound an inhibitory Na^+ ion at high Na^+ concentration to form an inactive ENa_3 or $EKNa_3$ complex. K^+ increased the affinity (by approximately 40-fold) of the site that bound the first Na^+ ion but did not affect the binding site for the second activating Na^+ ion, or the inhibitory site.

Tm-PPase differs from other membrane PPases in that the enzyme has the Asp residues Asp^{190} and Asp^{703} located in highly conserved regions at the predicted cytoplasm-membrane interfaces of loops *e* and *o*. To test whether the Asp residues participate in Na^+ binding, we substituted them to residues seen in phylogenetically related H^+-PPases that do not require Na^+ for activity. The Na^+-dose response curve of the D190A variant closely resembled that of the wild-type enzyme (Fig. 10). In contrast, the slope of the Na^+-dose response curve of the D703N variant was profoundly lower than the slope of the wild-type enzyme at all K^+ concentrations examined. Similarly, the K^+ activation profile of the D190A variant at fixed Na^+ concentrations resembled that of wild-type, whereas the profile of the D703N variant changed to become distinctly bell-shaped (Fig. 11). According to kinetic modeling, D703N substitution removed one of the two activating Na^+ binding sites, increased the binding affinity of the remaining activating Na^+ site, moderately increased the affinity of the activating K^+ binding site, and generated a new inhibitory K^+ binding site. K^+ ions modulated Na^+-activation of the D703N variant indicating that the substitution eliminated Na^+ binding to the site that was K^+-independent. Possibly, D703N substitution converted the activating Na^+ binding site to an inhibitory K^+ binding site. Because of these changes in alkali metal ion binding, the D703N variant reached maximal activity at an Na^+ concentration approximately 10-fold lower than required for maximal wild-type activity, but began to lose activity even at 5 mM Na^+, because of enhanced

Na^+ binding to the inhibitory site. The properties of the D190A/D703N double variant were similar to those of the D703N variant, except that Na^+ and K^+ ion binding affinities were approximately two-fold lower. Interestingly, both the double variant and the wild-type had similar PPase activities, whereas both the D190A and D703N variants showed two-fold lower activities. This compensatory effect in the double variant suggests that Asp^{190} and Asp^{703} are close to each other in the Tm-PPase structure. However, only Asp^{703} participates in Na^+ binding. Because the D703N variant retained a requirement of Na^+ for activity, Asp^{703} is not the sole determinant of Na^+ dependence in Tm-PPase.

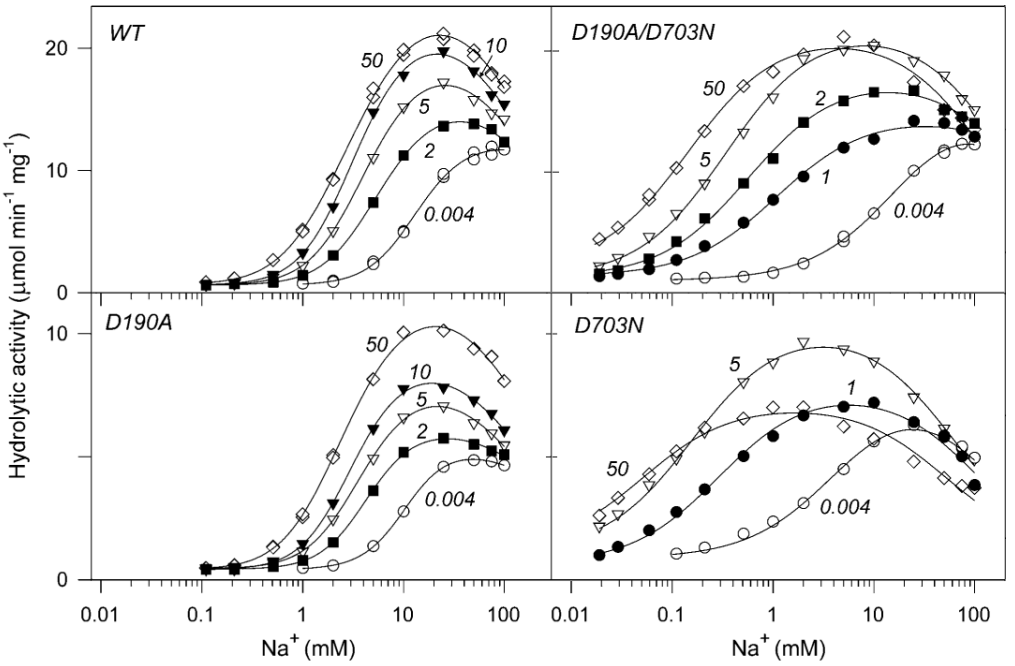

Figure 10 (modified from study II). Na^+ dependence of PP_i hydrolysis rates of wild-type and variant Tm-PPases in IMVs at fixed K^+ concentrations (shown on the curves in mM) at 40°C.

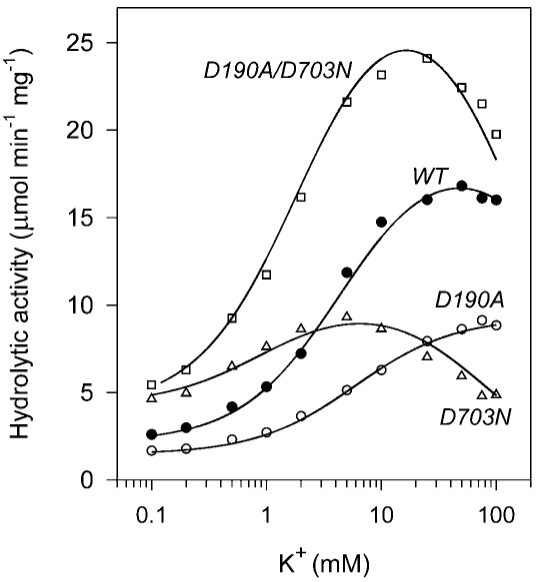

Figure 11 (study II). K^+ dependence of PP_i hydrolysis rates at a fixed Na^+ concentration of 5 mM for wild-type and variant Tm-PPases in IMVs at 40°C.

Purified Tm-PPase had low PP_i synthesis activity (0.9 nmol·min^{-1}·mg^{-1}), only 0.02% that of hydrolytic activity. We assayed the PP_i synthesis rate by incubating P_i with Tm-PPase in the presence of ATP-sulfurylase, which rapidly and quantitatively converts formed PP_i into ATP, subsequently measured using a sensitive luciferase assay (Nyren and Lundin 1985; Fabrichniy *et al.* 1997). The reaction established equilibrium between PP_i and P_i, and was thus distinct from energy-driven PP_i synthesis, which can raise the level of PP_i above equilibrium in membrane systems. The dependence of synthesis rate on Na^+ concentration indicated that, consistent with data on PP_i hydrolysis, at least one Na^+ ion activated and another inhibited PP_i synthesis. However, the large data scatter prevented us from assigning the Na^+ binding stoichiometry more precisely. Quite surprisingly, K^+ decreased the rate of PP_i synthesis. The rate of P_i/H_2O oxygen exchange was lower than the detection limit of our assay system (<5 nmol·min^{-1}·mg^{-1}). The slowness of the PP_i synthesis and oxygen exchange reactions may indicate tight coupling between these reactions and vectorial Na^+ transport.

4.2.4 Interactions between ion binding sites

K^+ binding to Mm-PPase and Tm-PPase profoundly stimulated the binding of Na^+ to enzyme, indicating significant functional interactions between the binding sites. To explore whether similar interactions existed between other ligand binding sites, we determined the rate of PP_i hydrolysis by Mm-PPase over a wide range of Mg^{2+}, Na^+, and Mg_2PP_i concentrations. To restrain the complexity of this multi-ligand system, we employed K^+ either at a saturating concentration or omitted the ion completely. By kinetic modeling, K^+ increased

Mg^{2+} binding affinity of both the free enzyme and the enzyme-substrate complex two-or-three-fold and decreased the substrate (Mg_2PP_i) binding affinity to a similar extent. These K^+-dependent changes in ligand binding properties are minor in comparison to the 10–40-fold stimulating effect of K^+ on Na^+ binding affinity, which appears to be the primary mechanism by which K^+ regulates Mm-PPase activity *in vivo*. The value of the apparent Michaelis constant (K_m^{app}) for substrate was almost independent of Mg^{2+} concentration (Fig. 8B), indicating that Mg^{2+} and substrate binding sites do not interact to a significant extent. In terms of Scheme 1, the observation is explained by the similarity of the $K_{A1}K_{A2}$ and $K_{M1}K_{M2}$ values (Table 2). K_m^{app} for Mg_2PP_i depended only weakly on Na^+ concentration (Fig. 12B), both in the presence and absence of K^+, indicating limited interaction between the substrate and the low affinity Na^+ binding site. The rate of substrate turnover (k_h^{app}) approached zero at low Na^+ levels, signifying that occupancy of the high- and low-affinity Na^+ binding sites is absolutely critical for catalytic function (Fig. 12B). More complex interrelationships between Mg^{2+} and Na^+ binding sites were evident in the enzyme–substrate complex. Accordingly, the two activating Na^+ ions bind to the Mg^{2+}-free enzyme in a positively cooperative manner, whereas the binding mode is normal (*i.e.,* Na^+ binds first to the higher affinity site) in the Mg^{2+}-bound form of the enzyme. In addition, Mm-PPase is susceptible to inhibition by excess Na^+, especially at low Mg^{2+} concentrations, which may mean that Na^+ is able to replace Mg^{2+} in one of the activating Mg^{2+} binding sites.

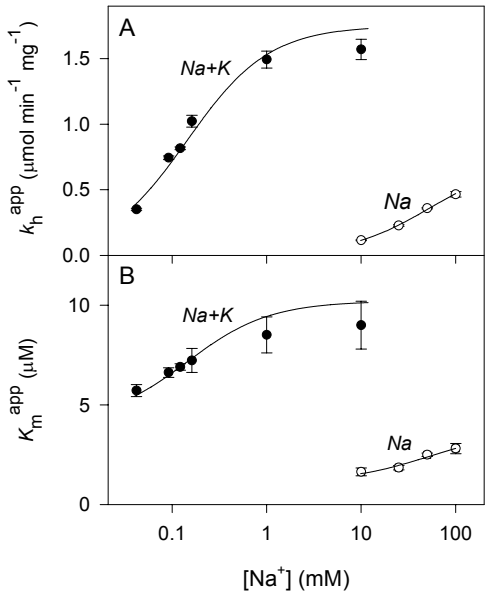

Figure 12 (study IV). Dependence of k_h^{app} (A) and K_m^{app} (for Mg_2PP_i) (B) values of Mm-PPase on Na^+ concentration. Measurements were performed in the presence of 5 mM free Mg^{2+}; the K^+ concentration was either zero (○) or 50 mM (●). Assays were performed at 25°C.

4.2.5 Conformational changes coupled to ligand binding

The SH reagent mersalyl inactivated Mm-PPase in a biphasic manner. The first phase resulted in an "immediate" loss of approximately 20% of activity. The second phase was resolved in time, and the rate constant varied several-fold depending on the nature of the ligands present (Fig. 13 A). Trypsin inactivated Mm-PPase in a simple monophasic manner (Fig. 13 B). The correlation between the effects of ligands on the two types of inactivation, caused by different chemical mechanisms, excluded the possibility that alterations in inactivation rates arose by direct interactions between ligands and inhibitors. The inactivation rate rather depended on accessibility of target residues (lysines, arginines, and cysteines) in the various enzyme–ligand complexes. Both mersalyl and trypsin are membrane-impermeable; ligand-induced changes in inactivation rate are therefore attributable to conformational changes in the cytoplasmic segment of Mm-PPase.

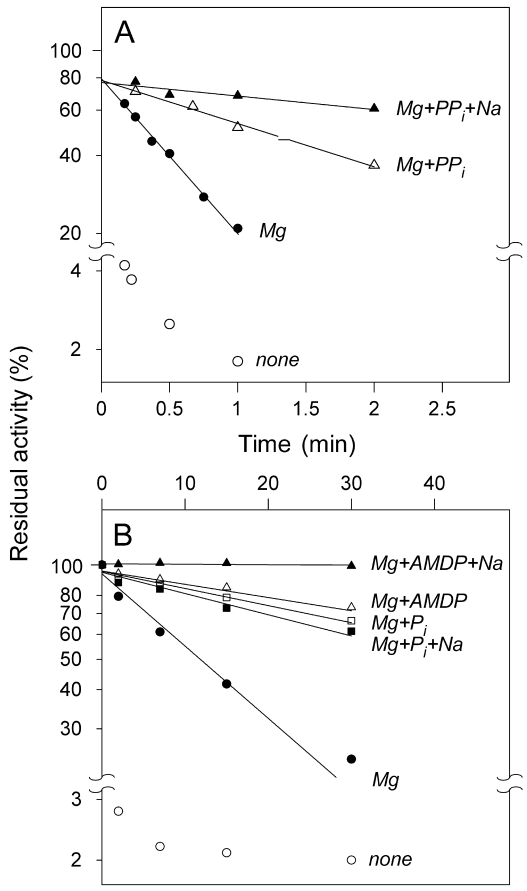

Figure 13 (study IV). Protection of Mm-PPase by different ligands upon 5 μM mersalyl (A) or 93 μg/mL trypsin (B) inactivation. The ligands were included at the concentrations indicated in Table 3.

When Mg^{2+} was omitted, Mm-PPase lost activity very rapidly, and none of Na^+, K^+, PP_i, or P_i had a protective effect. Mg^{2+} decelerated mersalyl and trypsin inactivation rates dramatically (Table 3). PP_i or the competitive inhibitor AMDP caused a further decrease in the inactivation rate of the enzyme–Mg^{2+} complex. We determined K_d for Mg_2PP_i in the absence of Na^+ and K^+ from residual activity after fixed-time incubations with mersalyl at variable Mg_2PP_i concentrations (Fig. 14). The value of K_d (7±1 μM; Table 3) agreed reasonably well with the Michaelis constant for PP_i hydrolysis and thus verified the conclusion drawn from steady-state kinetic measurements that Mm-PPase can bind substrate (Mg_2PP_i) in the absence of Na^+. Several other divalent cations (Ca^{2+}, Co^{2+}, Mn^{2+}, and Ni^{2+}) substituted for Mg^{2+} as a protecting ligand and mediated substrate binding. However, only Mn^{2+} could support low PP_i hydrolysis activity by Mm-PPase (~4% of Mg^{2+}-supported activity). The metal binding sites in the enzyme are therefore specific for Mg^{2+} at the catalytic but not at the binding level. Addition of Na^+ to the enzyme-substrate/AMDP complex triggered transition to the conformation most resistant to inactivation. K_d for the Na^+-triggered conformational change in the K^+-free enzyme–AMDP complex was 390±90 μM, in line with Na^+ binding to the high-affinity binding site identified by steady-state kinetics. The protection assay thus provides independent support for the suggested model involving two Na^+ binding sites. Na^+ as the sole ligand increased mersalyl inactivation only at high Na^+ concentrations (K_d of 300±30 mM). This effect may result from ion binding to the weak inhibitory Na^+ binding site identified by steady-state kinetics. The protective effect of P_i, the reaction product, was similar to that of PP_i or AMDP, with the exception that Na^+ did not further modulate the inactivation rate in the presence of P_i. P_i binding (K_d of 90±30 μM) was an order of magnitude weaker than PP_i binding. K^+ had a negligible effect on the inactivation rate of any ligand-enzyme complex.

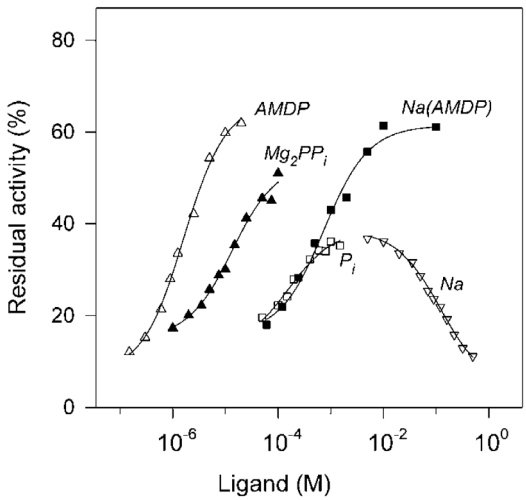

Figure 14 (modified from study III). Residual activity of Mm-PPase after incubation with mersalyl, as a function of ligand concentration. Curve labels indicate the ligand varied (without parentheses) and the fixed ligand(s) (in parentheses). Fixed ligand concentrations were saturating. Mersalyl concentrations and incubation times for different experimental curves were adjusted to obtain large variations in residual activities in response to changes in ligand concentrations.

Table 3 (study IV). Parameters describing effects of ligands on Mm-PPase inactivation by mersalyl and trypsin.

ligand(s)[a]	varied ligand	mersalyl		trypsin
		k^b (min^{-1})	$K_d{}^b$ (μM)	k (h^{-1})
None		> 20		>100
Mg^{2+}		1.35 ± 0.1		2.7 ± 0.2
Mg^{2+}, Na^+	Na^+	1.85 ± 0.1	300000 ± 30000	1.7 ± 0.1
Mg^{2+}, Na^+, K^+		1.45 ± 0.15		
Mg^{2+}, Mg_2PP_i	Mg_2PP_i	0.40 ± 0.05	7 ± 1	
Mg^{2+}, AMDP	AMDP	0.40 ± 0.05	0.8 ± 0.1	0.5 ± 0.1
Mg^{2+}, Na^+, AMDP	AMDP	0.15 ± 0.05		< 0.1
Mg^{2+}, Na^+, AMDP	Na^+	0.10 ± 0.05	390 ± 90	< 0.1
Mg^{2+}, P_i	P_i	0.45 ± 0.05	90 ± 30	0.7 ± 0.1
Mg^{2+}, Na^+, P_i		0.50 ± 0.05		0.8 ± 0.1

[a] Complete set of ligands present in the incubation medium. Ligand concentrations, except for the varied ligand in the K_d measurements, were 5 mM Mg^{2+}, 100 mM Na^+ (10 mM Na^+ when K^+ was present), 50 mM K^+, 200 μM Mg_2PP_i, 20 μM AMDP, and 1.5 mM P_i.
[b] Value for the varied ligand.

Our data on the steady-state kinetics and ligand protection of Mm-PPase provides the basis for a working model of Na^+-PPase function. Because other ligands afforded protection only in the presence of Mg^{2+}, and as Mg^{2+}-free enzyme was highly susceptible to inactivation, Mg^{2+} has a crucial structural role in organization of the cytoplasmic segment and the active site. The Mg^{2+} binding affinity is relatively high, suggesting that the enzyme is saturated by

Mg^{2+} *in vivo*. The substrate, Mg_2PP_i, is able to bind to the enzyme–Mg^{2+} complex in the absence of other ligands, causing a conformational change in the enzyme. However, only the successive binding of Na^+ to the high affinity site, which may represent the acceptor site for the transported ion, induces transition of the Na^+-PPase cytoplasmic segment to the most compact conformation. Importantly, both PP_i and its non-hydrolysable analogue AMDP showed similar protective effects, signifying that catalysis *per se* is not required for attainment of the most compact conformation. The compactness of the cytoplasmic segment continues until both P_i products are released from the active site and the enzyme relaxes to the initial conformation. Na^+ did not modulate the inactivation rate of the enzyme–P_i complex, which may reflect the inaccessibility, from the cytoplasm, of Na^+ binding sites when the enzyme is in this conformation. Therefore, PP_i binding and the release of P_i from the active site may serve as major triggers for changes in protein conformation that allow cyclic rotation of the Na^+ binding site relative to the membrane as part of the transport mechanism.

4.3 Site-directed mutagenesis of residues universally conserved in membrane PPases (study I)

To explore the functional and structural significance of residues universally conserved in membrane PPases, we chose to individually replace six Asp (187, 191, 642, 669, 673, and 677), four Glu (197, 202, 550, and 649), and three Lys (184, 195, and 646) residues in the cytoplasmic loops of *R. rubrum* H^+-transporting PPase (R-PPase) with Glu, Asp, or Arg, respectively (Fig. 15). R-PPase was chosen as a model enzyme because this is the best-characterized K^+-independent H^+-PPase. The substitutions did not affect expression of variant enzymes in *E. coli*, but, except for the Glu→Asp substitutions, inhibited R-PPase activity to a level indistinguishable from background (<5% of wild-type activity). This drastic decrease in enzyme activity signified the importance of the mutated Asp and Lys residues in catalysis, but precluded further studies using a kinetic approach. R-PPase tolerated Glu residue substitutions much better, and even E197A, E550A, and E649A variants retained 60%, 50%, and 20%, respectively, of wild-type activity. However, the E202A variant, in contrast to the Glu→Asp variant, had no activity. Substitution had no noticeable effect on the coupling efficiency of PP_i hydrolysis and H^+ transport in any active variant, consistent with localization of Glu residues in cytoplasmic loops. However, substitution of Glu^{263} and Glu^{233} (corresponding to Glu^{197} and Glu^{202} in R-PPase) in *V. radiata* (Nakanishi *et al.* 2001) and *S. coelicolor* (Hirono *et al.* 2007) H^+-PPases, respectively, decreased apparent coupling ratios. It is unlikely that the Glu residues are involved in proton transport in these enzymes and not in R-PPase. The Glu substitutions possibly caused partial decoupling in *V. radiata* and *S. coelicolor* H^+-PPases only indirectly, perhaps by disrupting more fragile overall enzyme structures. In

contrast, our data on indispensability of Asp^{187}, Asp^{191}, Asp^{669}, Asp^{673}, Asp^{677}, and Lys^{196} for catalytic activity of R-PPase is consistent with results from work with *V. radiata* and *S. coelicolor* H^+-PPases (Nakanishi *et al.* 2001; Hirono *et al.* 2007).

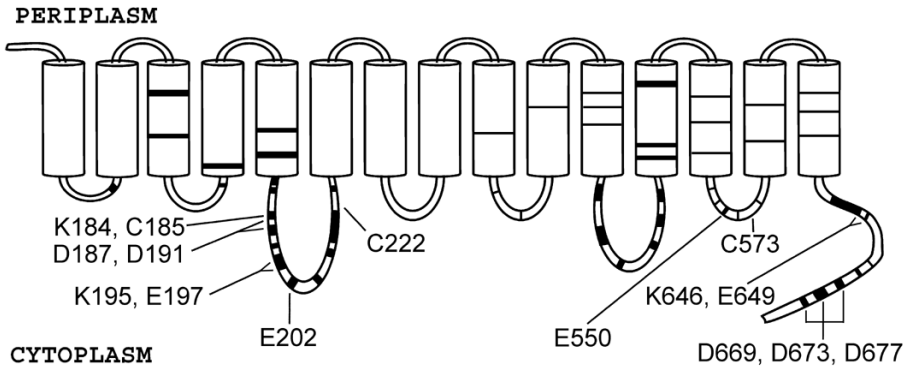

Figure 15 (modified from study I). A topological model of R-PPase as predicted from the amino acid sequence using the program TMHMM (Krogh *et al.* 2001). The prediction is fully compatible with the experimental topological model of *S. coelicolor* H^+-PPase. The approximate positions of identical amino acid residues in the membrane PPase family are depicted in black. The substituted residues and mersalyl-reactive cysteine residues are indicated.

Steady-state kinetic analysis of Glu→Asp variants performed over a wide range of Mg^{2+} concentrations indicated a common decrease in catalytic efficiency (signified by k_h^{app}/K_m^{app} ratio), compared to that of wild-type R-PPase, at low Mg^{2+} concentrations (<0.5 mM). By kinetic modeling, the observation is explained by PP_i hydrolysis by the variant enzyme via the EMg_3PP_i complex only. In contrast, the wild-type enzyme additionally hydrolyzes PP_i in the EMg_2PP_i complex. In the absence of the conserved Glu, two Mg^{2+} ions appear insufficient to form a catalytically competent active site structure, which is restored only upon binding of a third Mg^{2+} ion. Additionally, the substrate (Mg_2PP_i) binds to a preformed enzyme-Mg^{2+} complex.

Steady-state kinetic modeling of E197D, E202D, and E649D variants suggested 3–35-fold decreases in binding affinities of the high-affinity Mg^{2+} site in the substrate-free enzyme. However, no such significant change was observed when the binding constant was estimated from protection afforded by Mg^{2+} against enzyme inactivation by mersalyl. This discrepancy may result from the fact that the inhibitor approach provides a measure of overall metal binding, whereas kinetics report on only functional binding. The protein structure is flexible, allowing for efficient metal binding to even variant enzymes, but most resulting complexes may be non-productive because metals

are mispositioned. A similar pattern is well documented for soluble PPases (Hyytia *et al.* 2001; Pohjanjoki *et al.* 2001). Additional functional defects in variant enzymes included changes in pK_a values of the E649D variant resulting in a narrow pH optimum range for enzyme activity. The observed decrease in binding affinities of the substrate analogues AMDP and methylenediphosphonate to E197D, E202D, and E649D variants suggests impaired PP_i binding to these enzymes.

E550D and E649D variants reacted 40- and 4-fold more rapidly, respectively, with mersalyl than did the wild-type enzyme, suggesting that the substitutions resulted in structural changes in the enzyme. R-PPase contains three mersalyl-reactive Cys residues (Belogurov *et al.* 2002b). To simplify analysis, we eliminated the contribution of Cys^{185} by engineering an additional C185G substitution in the variant enzymes, corresponding to a naturally occurring isoform. Cys^{222} is involved in the "immediate" phase of inactivation that typically eliminates ~20% of PPase activity, whereas the Cys^{573} reaction is responsible for the slower time-resolved inhibition culminating in complete inactivation. In agreement with the above assignment, substitutions (E550D and E649D) in the vicinity of Cys^{573} increased the rate constant of the time-resolved mersalyl inactivation step, whereas substitutions (E197D and E202D) close to Cys^{222} had no significant effects. We therefore suggest that perturbation of R-PPase structure by E550D and E649D substitutions indirectly caused increases in solvent accessibility and thus in mersalyl reactivity of the Cys^{573} residue.

In conclusion, membrane PPase flexibility results in functional defects even in conservatively substituted variant enzymes. Distinguishing between direct and indirect effects of amino acid substitutions will be possible when the three-dimensional structure of membrane PPase is determined.

ACKNOWLEDGMENTS

This study was carried out during 2002–2008 at the Department of Biochemistry and Food Chemistry at the University of Turku, Finland. I was also fortunate to be a student in a wonderful National Graduate School in Informational and Structural Biology (ISB). The study was funded by the University of Turku, ISB, the Emil Aaltonen Foundation, and the Turku University Foundation, all of which are acknowledged. I also thank Professors Mark S. Johnson and Masayoshi Maeshima for critically reviewing my thesis and Professor Aurelio Serrano for acting as an opponent in the dissertation.

Importantly, I want to thank Professors Reijo Lahti and Alexander Baykov for supervising my Ph.D. thesis project; their balance of scientific guidance and respect for my research freedom suiting me perfectly. Dr. Georgiy Belogurov, my former M.Sc. research project supervisor, colleague, and co-author, excelled in tutoring me in the practice of science at the bench and set an excellent example that has guided my path to graduation. I acknowledge the current and former members of the PPase laboratory: Dr. Anu Salminen, Dr. Pasi Halonen, Dr. Marko Tammenkoski, Heidi Tuominen, and Joonas Jämsén, and thank them for sharing their scientific expertise with me. I thank Professor Jyrki Heino for providing an excellent research environment at the Department of Biochemistry. Jani Sointusalo has skillfully maintained our scientific instruments, whereas Anu Hirvensalo and Pirkko Haavisto have saved me lots of time by taking care of laboratory chemicals and glassware. Similarly, our efficient secretary Satu Jasu has kindly minimized my direct involvement in bureaucratic paper shuffling.

My parallel role as a teacher in our Department has provided me many enlightening opportunities to serve as a tutor and spokesman for biochemistry. I thank students for sharing their interest in life in molecular and atomic detail. I am especially grateful to my talented M.Sc. research project students Heidi Luoto, Kati Kemppainen, Joonas Jämsén, Piia-Riitta Karhemo, and Alicia Rodriguez Folgueras. The fact that they will continue to succeed in science gives me great satisfaction.

I sincerely thank my many dear friends for growing up with me, playing, studying, traveling, partying, and sharing their lives with me. A life without friends is no life. I further acknowledge the members of my football team KuuLa for lining up beside me in the field, where we shared incredibly strong feelings of joy and despair.

My mother Mirja and father Reijo have always fully supported my slow ascent of the educational ladder. I thank them and my siblings Tiina, Mikko, and Tuomas. Very importantly, I thank my wife Anna-Leena for her support and love. The third member of our tribe, an always cheerful labrador retriever Onni, deserves thanks for his companionship.

Turku, April 2009

Anssi Malinen

REFERENCES

Altschul, S.F., Gish, W., Miller, W., Myers, E.W. and Lipman, D.J. (1990). Basic local alignment search tool. *J Mol Biol* **215**(3): 403-410.

Au, K.M., Barabote, R.D., Hu, K.Y. and Saier, M.H., Jr. (2006). Evolutionary appearance of H^+-translocating pyrophosphatases. *Microbiology* **152**(Pt 5): 1243-1247.

Ballesteros, E., Donaire, J.P. and Belver, A. (1996). Effects of salt stress on H^+-ATPase and H^+-PPase activities of tonoplast-enriched vesicles isolated from sunflower roots. *Physiologia Plantarum* **97**(2): 259-268.

Baltscheffsky, H., Von Stedingk, L.V., Heldt, H.W. and Klingenberg, M. (1966). Inorganic pyrophosphate: formation in bacterial photophosphorylation. *Science* **153**(740): 1120-1122.

Baltscheffsky, M. (1967). Inorganic pyrophosphate and ATP as energy donors in chromatophores from *Rhodospirillum rubrum*. *Nature* **216**(5112): 241-243.

Baltscheffsky, M. and Nyrén, P. (1986). Preparation and reconstitution of the proton-pumping membrane-bound inorganic pyrophosphatase from *Rhodospirillum rubrum*. *Methods Enzymol* **126**: 538-545.

Baltscheffsky, M., Schultz, A. and Baltscheffsky, H. (1999). H^+-PPases: a tightly membrane-bound family. *FEBS Lett* **457**(3): 527-533.

Baumer, S., Lentes, S., Gottschalk, G. and Deppenmeier, U. (2002). Identification and analysis of proton-translocating pyrophosphatases in the methanogenic archaeon *Methansarcina mazei*. *Archaea* **1**(1): 1-7.

Baykov, A.A. and Avaeva, S.M. (1981). A simple and sensitive apparatus for continuous monitoring of orthophosphate in the presence of acid-labile compounds. *Anal Biochem* **116**(1): 1-4.

Baykov, A.A., Dubnova, E.B., Bakuleva, N.P., Evtushenko, O.A., Zhen, R.G. and Rea, P.A. (1993a). Differential sensitivity of membrane-associated pyrophosphatases to inhibition by diphosphonates and fluoride delineates two classes of enzyme. *FEBS Lett* **327**(2): 199-202.

Baykov, A.A., Bakuleva, N.P. and Rea, P.A. (1993b). Steady-state kinetics of substrate hydrolysis by vacuolar H(+)-pyrophosphatase. A simple three-state model. *Eur J Biochem* **217**(2): 755-762.

Baykov, A.A., Kasho, V.N., Bakuleva, N.P. and Rea, P.A. (1994). Oxygen exchange reactions catalyzed by vacuolar H(+)-translocating pyrophosphatase. Evidence for reversible formation of enzyme-bound pyrophosphate. *FEBS Lett* **350**(2-3): 323-327.

Baykov, A.A., Sergina, N.V., Evtushenko, O.A. and Dubnova, E.B. (1996a). Kinetic characterization of the hydrolytic activity of the H^+-pyrophosphatase of *Rhodospirillum rubrum* in membrane-bound and isolated states. *Eur J Biochem* **236**(1): 121-127.

Baykov, A.A., Hyytia, T., Volk, S.E., Kasho, V.N., Vener, A.V., Goldman, A., Lahti, R. and Cooperman, B.S. (1996b). Catalysis by *Escherichia coli* inorganic pyrophosphatase: pH and Mg^{2+} dependence. *Biochemistry* **35**(15): 4655-4661.

Baykov, A.A., Cooperman, B.S., Goldman, A. and Lahti, R. (1999). Cytoplasmic inorganic pyrophosphatase. *Prog Mol Subcell Biol* **23**: 127-150.

Baykov, A.A., Fabrichniy, I.P., Pohjanjoki, P., Zyryanov, A.B. and Lahti, R. (2000). Fluoride effects along the reaction pathway of pyrophosphatase: Evidence for a second enzyme center dot pyrophosphate intermediate. *Biochemistry* **39**(39): 11939-11947.

Becker, A., Canut, H., Luttge, U., Maeshima, M., Marigo, G. and Ratajczak, R. (1995). Purification and immunological comparison of the tonoplast H^+-pyrophosphatase from cells of *Catharanthus roseus* and leaves from *Mesembryanthemum crystallinum* performing C-3-photosynthesis and the obligate CAM-plant *Kalanchoe daigremontiana*. *J Plant Physiol* **146**(1-2): 88-94.

Belogurov, G.A. and Lahti, R. (2002a). A lysine substitute for K^+. A460K mutation eliminates K^+ dependence in H^+-pyrophosphatase of *Carboxydothermus hydrogenoformans*. *J Biol Chem* **277**(51): 49651-49654.

Belogurov, G.A., Turkina, M.V., Penttinen, A., Huopalahti, S., Baykov, A.A. and Lahti, R. (2002b). H^+-pyrophosphatase of *Rhodospirillum rubrum*: High-yield expression in *Escherichia coli* and identification of the Cys residues responsible for inactivation by mersalyl. *J Biol Chem* **277**(25): 22209-22214.

Belogurov, G.A. (2004). Pyrophosphate-energized proton pumps: identification of the residues determining K^+ requirements and discovery of a Na^+-dependent enzyme. *PhD. Thesis,* Department of Biochemistry and Food Chemistry, University of Turku, Finland.

Berkich, D.A., Williams, G.D., Masiakos, P.T., Smith, M.B., Boyer, P.D. and LaNoue, K.F. (1991). Rates of various reactions catalyzed by ATP synthase as related to the mechanism of ATP synthesis. *J Biol Chem* **266**(1): 123-129.

Besteiro, S., Tonn, D., Tetley, L., Coombs, G.H. and Mottram, J.C. (2008). The AP3 adaptor is involved in the transport of membrane proteins to acidocalcisomes of Leishmania. *J Cell Sci* **121**(Pt 5): 561-570.

Bowie, J.U. (2005). Solving the membrane protein folding problem. *Nature* **438**(7068): 581-589.

Bradford, M.M. (1976). A rapid and sensitive method for the quantitation of microgram quantities of protein utilizing the principle of protein-dye binding. *Anal Biochem* **72**: 248-254.

Britten, C.J., Turner, J.C. and Rea, P.A. (1989). Identification and purification of substrate-binding subunit of higher-plant H^+-translocating inorganic pyrophosphatase. *FEBS Letters* **256**(1-2): 200-206.

Britten, C.J., Zhen, R.G., Kim, E.J. and Rea, P.A. (1992). Reconstitution of transport function of vacuolar H(+)-translocating inorganic pyrophosphatase. *J Biol Chem* **267**(30): 21850-21855.

Carystinos, G.D., MacDonald, H.R., Monroy, A.F., Dhindsa, R.S. and Poole, R.J. (1995). Vacuolar H(+)-translocating pyrophosphatase is induced by anoxia or chilling in seedlings of rice. *Plant Physiol* **108**(2): 641-649.

Chanson, A., Fichmann, J., Spear, D. and Taiz, L. (1985). Pyrophosphate-driven proton transport by microsomal membranes of corn coleoptiles. *Plant Physiol* **79**(1): 159-164.

Chen, G., Gharib, T.G., Huang, C.C., Thomas, D.G., Shedden, K.A., Taylor, J.M., Kardia, S.L., Misek, D.E., Giordano, T.J., Iannettoni, M.D., Orringer, M.B., Hanash, S.M. and Beer, D.G. (2002). Proteomic analysis of lung adenocarcinoma: identification of a highly expressed set of proteins in tumors. *Clin Cancer Res* **8**(7): 2298-2305.

Colombo, R. and Cerana, R. (1993). Enhanced activity of tonoplast pyrophosphatase in NaCl-grown cells of *Daucus carota*. *J Plant Physiol* **142**(2): 226-229.

Davies, J.M., Rea, P.A. and Sanders, D. (1991). Vacuolar proton-pumping pyrophosphatase in *Beta vulgaris* shows vectorial activation by potassium. *FEBS Lett* **278**(1): 66-68.

Davies, J.M., Poole, R.J., Rea, P.A. and Sanders, D. (1992). Potassium transport into plant vacuoles energized directly by a proton-pumping inorganic pyrophosphatase. *Proc Natl Acad Sci U S A* **89**(24): 11701-11705.

Davies, J.M., Poole, R.J. and Sanders, D. (1993). The computed free-energy change of hydrolysis of inorganic pyrophosphate and ATP – apparent significance for inorganic-pyrophosphate-driven reactions of intermediary metabolism. *Biochim Biophys Acta* **1141**(1): 29-36.

de Graaf, B.H., Rudd, J.J., Wheeler, M.J., Perry, R.M., Bell, E.M., Osman, K., Franklin, F.C. and Franklin-Tong, V.E. (2006). Self-incompatibility in Papaver targets soluble inorganic pyrophosphatases in pollen. *Nature* **444**(7118): 490-493.

Dimroth, P. and Cook, G.M. (2004). Bacterial Na^+- or H^+-coupled ATP synthases operating at low electrochemical potential. *Adv Microb Physiol* **49**: 175-218.

Docampo, R., de Souza, W., Miranda, K., Rohloff, P. and Moreno, S.N. (2005). Acidocalcisomes - conserved from bacteria to man. *Nat Rev Microbiol* **3**(3): 251-261.

Docampo, R. and Moreno, S.N. (2008). The acidocalcisome as a target for chemotherapeutic agents in protozoan parasites. *Curr Pharm Des* **14**(9): 882-888.

Drake, H.L. and Daniel, S.L. (2004). Physiology of the thermophilic acetogen *Moorella thermoacetica*. *Res Microbiol* **155**(10): 869-883.

Drake, R., Serrano, A. and Perez-Castineira, J.R. (2004). Heterologous expression of membrane-bound inorganic pyrophosphatases in *Saccharomyces cerevisiae* is significantly improved by constructing chimeras with the N-terminal domain of *Trypanosoma cruzi* H^+-PPase. *Proceedings of the 3rd international meeting on inorganic pyrophosphatases*, 56-59, The University of Birmingham, UK.

Drozdowicz, Y.M., Lu, Y.P., Patel, V., Fitz-Gibbon, S., Miller, J.H. and Rea, P.A. (1999). A thermostable vacuolar-type membrane pyrophosphatase from the archaeon *Pyrobaculum aerophilum*: implications for the origins of pyrophosphate-energized pumps. *FEBS Lett* **460**(3): 505-512.

Drozdowicz, Y.M., Kissinger, J.C. and Rea, P.A. (2000). AVP2, a sequence-divergent, K(+)-insensitive H(+)-translocating inorganic pyrophosphatase from Arabidopsis. *Plant Physiol* **123**(1): 353-362.

Drozdowicz, Y.M. and Rea, P.A. (2001). Vacuolar H(+) pyrophosphatases: from the evolutionary backwaters into the mainstream. *Trends Plant Sci* **6**(5): 206-211.

Drozdowicz, Y.M., Shaw, M., Nishi, M., Striepen, B., Liwinski, H.A., Roos, D.S. and Rea, P.A. (2003). Isolation and characterization of TgVP1, a type I vacuolar H^+-translocating pyrophosphatase from *Toxoplasma gondii*. The dynamics of its subcellular localization and the cellular effects of a diphosphonate inhibitor. *J Biol Chem* **278**(2): 1075-1085.

Duan, X.G., Yang, A.F., Gao, F., Zhang, S.L. and Zhang, J.R. (2007). Heterologous expression of vacuolar H(+)-PPase enhances the electrochemical gradient across the vacuolar membrane and improves tobacco cell salt tolerance. *Protoplasma* **232**(1-2): 87-95.

D'yakova, E.V., Rakitin, A.L., Kamionskaya, A.M., Baikov, A.A., Lahti, R., Ravin, N.V. and Skryabin, K.G. (2006). A study of the effect of expression of the gene encoding the membrane H^+-pyrophosphatase of *Rhodospirillum rubrum* on salt resistance of transgenic tobacco plants. *Dokkady Biol Sci* **409**: 346-348.

Fabrichniy, I.P., Kasho, V.N., Hyytia, T., Salminen, T., Halonen, P., Dudarenkov, V.Y., Heikinheimo, P., Chernyak, V.Y., Goldman, A., Lahti, R., Cooperman, B.S. and Baykov, A.A. (1997). Structural and functional consequences of substitutions at the tyrosine 55-lysine 104 hydrogen bond in *Escherichia coli* inorganic pyrophosphatase. *Biochemistry* **36**(25): 7746-7753.

Facanha, A.R. and de Meis, L. (1998). Reversibility of H(+)-ATPase and H(+)-pyrophosphatase in tonoplast vesicles from maize coleoptiles and seeds. *Plant Physiol* **116**(4): 1487-1495.

Fang, J., Rohloff, P., Miranda, K. and Docampo, R. (2007). Ablation of a small transmembrane protein of *Trypanosoma brucei* (TbVTC1) involved in the synthesis of polyphosphate alters acidocalcisome biogenesis and function, and leads to a cytokinesis defect. *Biochem J* **407**(2): 161-170.

Fraichard, A., Magnin, T., Trossat, C. and Pugin, A. (1993). Properties of the proton-pumping pyrophosphatase in tonoplast vesicles of *Acer pseudoplatanus* – functional molecular-mass and polypeptide composition. *Plant Physiol Biochem* **31**(3): 349-359.

Fraichard, A., Trossat, C., Perotti, E. and Pugin, A. (1996). Allosteric regulation by Mg^{2+} of the vacuolar H(+)-PPase from *Acer pseudoplatanus* cells. Ca^{2+}/Mg^{2+} interactions. *Biochimie* **78**(4): 259-266.

Fukuda, A., Chiba, K., Maeda, M., Nakamura, A., Maeshima, M. and Tanaka, Y. (2004). Effect of salt and osmotic stresses on the expression of genes for the vacuolar H^+-pyrophosphatase, H^+-ATPase subunit A, and Na^+/H^+ antiporter from barley. *J Exp Bot* **55**(397): 585-594.

Fukuda, A. and Tanaka, Y. (2006). Effects of ABA, auxin, and gibberellin on the expression of genes for vacuolar H^+-inorganic pyrophosphatase, H^+-ATPase subunit A, and Na^+/H^+ antiporter in barley. *Plant Physiol Biochem* **44**(5-6): 351-358.

Gao, F., Gao, Q., Duan, X., Yue, G., Yang, A. and Zhang, J. (2006). Cloning of an H^+-PPase gene from *Thellungiella halophila* and its heterologous expression to improve tobacco salt tolerance. *J Exp Bot* **57**(12): 3259-3270.

Garcia-Contreras, R., Celis, H. and Romero, I. (2004). Importance of *Rhodospirillum rubrum* H(+)-pyrophosphatase under low-energy conditions. *J Bacteriol* **186**(19): 6651-6655.

Gaxiola, R.A., Rao, R., Sherman, A., Grisafi, P., Alper, S.L. and Fink, G.R. (1999). The *Arabidopsis thaliana* proton transporters, AtNhx1 and Avp1, can function in cation detoxification in yeast. *Proc Natl Acad Sci U S A* **96**(4): 1480-1485.

Gaxiola, R.A., Li, J., Undurraga, S., Dang, L.M., Allen, G.J., Alper, S.L. and Fink, G.R. (2001). Drought- and salt-tolerant plants result from overexpression of the AVP1 H^+-pump. *Proc Natl Acad Sci U S A* **98**(20): 11444-11449.

Gaxiola, R.A., Palmgren, M.G. and Schumacher, K. (2007). Plant proton pumps. *FEBS Lett* **581**(12): 2204-2214.

Gomez-Garcia, M.R., Losada, M. and Serrano, A. (2003). Concurrent transcriptional activation of ppa and ppx genes by phosphate deprivation in the cyanobacterium *Synechocystis sp.* strain PCC 6803. *Biochem Biophys Res Commun* **302**(3): 601-609.

Gordon-Weeks, R., Steele, S.H. and Leigh, R.A. (1996). The role of magnesium, pyrophosphate, and their complexes as substrates and activators of the vacuolar H^+-pumping inorganic pyrophosphatase – studies using ligand protection from covalent inhibitors. *Plant Physiol* **111**(1): 195-202.

Gordon-Weeks, R., Koren'kov, V.D., Steele, S.H. and Leigh, R.A. (1997). Tris is a competitive inhibitor of K^+ activation of the vacuolar H^+-pumping pyrophosphatase. *Plant Physiol* **114**(3): 901-905.

Gordon-Weeks, R., Parmar, S., Davies, T.G. and Leigh, R.A. (1999). Structural aspects of the effectiveness of bisphosphonates as competitive inhibitors of the plant vacuolar proton-pumping pyrophosphatase. *Biochem J* **337**(Pt 3): 373-377.

Guillory, R.J. and Fisher, R.R. (1972). Studies on light-dependent synthesis of inorganic pyrophosphate by *Rhodospirillum rubrum* chromatophores. *Biochem J* **129**(2): 571-581.

Gulick, P.J., Drouin, S., Yu, Z., Danyluk, J., Poisson, G., Monroy, A.F. and Sarhan, F. (2005). Transcriptome comparison of winter and spring wheat responding to low temperature. *Genome* **48**(5): 913-923.

Guo, S., Yin, H., Zhang, X., Zhao, F., Li, P., Chen, S., Zhao, Y. and Zhang, H. (2006). Molecular cloning and characterization of a vacuolar H^+-pyrophosphatase gene, SsVP, from the halophyte *Suaeda salsa* and its overexpression increases salt and drought tolerance of Arabidopsis. *Plant Mol Biol* **60**(1): 41-50.

Harvey, G.W. and Keister, D.L. (1981). Energy-linked reactions in photosynthetic bacteria - P_i reversible H_2O oxygen-exchange catalyzed by the membrane-bound inorganic pyrophosphatase of *Rhodospirillum rubrum*. *Arch Biochem Biophys* **208**(2): 426-430.

Hedlund, J., Cantoni, R., Baltscheffsky, M., Baltscheffsky, H. and Persson, B. (2006). Analysis of ancient sequence motifs in the H^+-PPase family. *FEBS J* **273**(22): 5183-5193.

Hedrich, R., Kurkdjian, A., Guern, J. and Flugge, U.I. (1989). Comparative studies on the electrical properties of the H^+-translocating ATPase and pyrophosphatase of the vacuolar-lysosomal compartment. *EMBO J* **8**(10): 2835-2841.

Heinonen, J.K. (2001). Biological role of inorganic pyrophosphate. Kluwer Academic Publishers, London.

Hill, J.E., Scott, D.A., Luo, S. and Docampo, R. (2000). Cloning and functional expression of a gene encoding a vacuolar-type proton-translocating pyrophosphatase from *Trypanosoma cruzi*. *Biochem J* **351**(Pt 1): 281-288.

Hirono, M., Mimura, H., Nakanishi, Y. and Maeshima, M. (2005). Expression of functional *Streptomyces coelicolor* H^+-pyrophosphatase and characterization of its molecular properties. *J Biochem (Tokyo)* **138**(2): 183-191.

Hirono, M., Nakanishi, Y. and Maeshima, M. (2007). Essential amino acid residues in the central transmembrane domains and loops for energy coupling of *Streptomyces coelicolor* A3(2) H^+-pyrophosphatase. *Biochim Biophys Acta* **1767**(7): 930-939.

Hirono, M., Nakanishi, Y. and Maeshima, M. (2007). Identification of amino acid residues participating in the energy coupling and proton transport of *Streptomyces coelicolor* A3(2) H^+-pyrophosphatase. *Biochim Biophys Acta* **1767**(12): 1401-1411.

Hsiao, Y.Y., Van, R.C., Hung, H.H. and Pan, R.L. (2002). Diethylpyrocarbonate inhibition of vacuolar H^+-pyrophosphatase possibly involves a histidine residue. *J Protein Chem* **21**(1): 51-58.

Hsiao, Y.Y., Van, R.C., Hung, S.H., Lin, H.H. and Pan, R.L. (2004). Roles of histidine residues in plant vacuolar H(+)-pyrophosphatase. *Biochim Biophys Acta* **1608**(2-3): 190-199.

Hsiao, Y.Y., Pan, Y.J., Hsu, S.H., Huang, Y.T., Liu, T.H., Lee, C.H., Liu, P.F., Chang, W.C., Wang, Y.K., Chien, L.F. and Pan, R.L. (2007). Functional roles of arginine residues in mung bean vacuolar H^+-pyrophosphatase. *Biochim Biophys Acta* **1767**(7): 965-973.

Huang, S., Colmer, T.D. and Millar, A.H. (2008). Does anoxia tolerance involve altering the energy currency towards PP_i? *Trends Plant Sci* **13**(5): 221-227.

Hyytia, T., Halonen, P., Salminen, A., Goldman, A., Lahti, R. and Cooperman, B.S. (2001). Ligand binding sites in *Escherichia coli* inorganic pyrophosphatase: effects of active site mutations. *Biochemistry* **40**(15): 4645-4653.

Ikeda, M., Satoh, S., Maeshima, M., Mukohata, Y. and Moritani, C. (1991). A vacuolar ATPase and pyrophosphatase in *Acetabularia acetabulum*. *Biochim Biophys Acta* **1070**(1): 77-82.

Ikeda, M., Umami, K., Hinohara, M., Tanimura, Y., Ohmae, A., Nakanishi, Y. and Maeshima, M. (2002). Functional expression of *Acetabularia acetabulum* vacuolar H(+)-pyrophosphatase in a yeast VMA3-deficient strain. *J Exp Bot* **53**(378): 2273-2275.

Jämsén, J., Tuominen, H., Salminen, A., Belogurov, G.A., Magretova, N.N., Baykov, A.A. and Lahti, R. (2007). A CBS domain-containing pyrophosphatase of *Moorella thermoacetica* is regulated by adenine nucleotides. *Biochem J*. **408**(3):327-333.

Johannes, E. and Felle, H. (1990). Proton Gradient across the tonoplast of *Riccia fluitans* as a result of the joint action of two electroenzymes. *Plant Physiology* **93**(2): 412-417.

Karlsson, J. (1975). Membrane-bound potassium and magnesium ion-stimulated inorganic pyrophosphatase from roots and cotyledons of sugar beet (*Beta vulgaris L*). *Biochim Biophys Acta* **399**(2): 356-363.

Keister, D.L. and Raveed, N.J. (1974). Energy-linked reactions in photosynthetic bacteria. P_i-PP_i exchange in *Rhodospirillum rubrum*. *Journal of Biological Chemistry* **249**(20): 6454-6458.

Kim, E.J., Zhen, R.G. and Rea, P.A. (1994). Heterologous expression of plant vacuolar pyrophosphatase in yeast demonstrates sufficiency of the substrate-binding subunit for proton transport. *Proc Natl Acad Sci U S A* **91**(13): 6128-6132.

Kim, E.J., Zhen, R.G. and Rea, P.A. (1995). Site-directed mutagenesis of vacuolar H(+)-pyrophosphatase. Necessity of Cys634 for inhibition by maleimides but not catalysis. *J Biol Chem* **270**(6): 2630-2635.

Krogh, A., Larsson, B., von Heijne, G. and Sonnhammer, E.L. (2001). Predicting transmembrane protein topology with a hidden Markov model: application to complete genomes. *J Mol Biol* **305**(3): 567-580.

Kuhla, B., Kuhla, S., Rudolph, P.E., Albrecht, D. and Metges, C.C. (2007). Proteomics analysis of hypothalamic response to energy restriction in dairy cows. *Proteomics* **7**(19): 3602-3617.

Kurilova, S.A., Bogdanova, A.V., Nazarova, T.I. and Avaeva, S.M. (1984). Changes in the *Escherichia coli* inorganic pyrophosphatase activity on interactions with magnesium, zinc, calcium and fluoride ions. *Bioorganicheskaya Khimiya* **10**(9): 1153-1160.

Laemmli, U.K. (1970). Cleavage of structural proteins during the assembly of the head of bacteriophage T4. *Nature* **227**(5259): 680-685.

Laubinger, W. and Dimroth, P. (1989). The sodium ion translocating adenosinetriphosphatase of *Propionigenium modestum* pumps protons at low sodium ion concentrations. *Biochemistry* **28**(18): 7194-7198.

Leigh, R.A., Pope, A.J., Jennings, I.R. and Sanders, D. (1992). Kinetics of the vacuolar H^+-pyrophosphatase - the roles of magnesium, pyrophosphate, and their complexes as substrates, activators, and inhibitors. *Plant Physiol* **100**(4): 1698-1705.

Lemercier, G., Dutoya, S., Luo, S., Ruiz, F.A., Rodrigues, C.O., Baltz, T., Docampo, R. and Bakalara, N. (2002). A vacuolar-type H^+-pyrophosphatase governs maintenance of functional acidocalcisomes and growth of the insect and mammalian forms of *Trypanosoma brucei*. *J Biol Chem* **277**(40): 37369-37376.

Lexander, H., Palmberg, C., Auer, G., Hellstrom, M., Franzen, B., Jornvall, H. and Egevad, L. (2005). Proteomic analysis of protein expression in prostate cancer. *Anal Quant Cytol Histol* **27**(5): 263-272.

Li, B., Wei, A., Song, C., Li, N. and Zhang, J. (2008). Heterologous expression of the TsVP gene improves the drought resistance of maize. *Plant Biotechnol J* **6**(2): 146-159.

Li, J., Yang, H., Peer, W.A., Richter, G., Blakeslee, J., Bandyopadhyay, A., Titapiwantakun, B., Undurraga, S., Khodakovskaya, M., Richards, E.L., Krizek, B., Murphy, A.S., Gilroy, S. and Gaxiola, R. (2005). Arabidopsis H^+-PPase AVP1 regulates auxin-mediated organ development. *Science* **310**(5745): 121-125.

Lin, H.H., Pan, Y.J., Hsu, S.H., Van, R.C., Hsiao, Y.Y., Chen, J.H. and Pan, R.L. (2005). Deletion mutation analysis on C-terminal domain of plant vacuolar H(+)-pyrophosphatase. *Arch Biochem Biophys* **442**(2): 206-213.

Lomax, T.L., Mehlhorn, R.J. and Briggs, W.R. (1985). Active auxin uptake by zucchini membrane vesicles: quantitation using ESR volume and delta pH determinations. *Proc Natl Acad Sci U S A* **82**(19): 6541-6545.

Long, A.R., Williams, L.E., Nelson, S.J. and Hall, J.L. (1995). Localization of membrane pyrophosphatase activity in *Ricinus communis* seedlings. *J Plant Physiol* **146**(5-6): 629-638.

Lopez-Marques, R.L., Perez-Castineira, J.R., Losada, M. and Serrano, A. (2004). Differential regulation of soluble and membrane-bound inorganic pyrophosphatases in the photosynthetic bacterium *Rhodospirillum rubrum* provides insights into pyrophosphate-based stress bioenergetics. *J Bacteriol* **186**(16): 5418-5426.

Lopez-Marques, R.L., Perez-Castineira, J.R., Buch-Pedersen, M.J., Marco, S., Rigaud, J.L., Palmgren, M.G. and Serrano, A. (2005). Large-scale purification of the proton pumping pyrophosphatase from *Thermotoga maritima*: a "Hot-Solve" method for isolation of recombinant thermophilic membrane proteins. *Biochim Biophys Acta* **1716**(1): 69-76.

Luo, S., Marchesini, N., Moreno, S.N. and Docampo, R. (1999). A plant-like vacuolar H(+)-pyrophosphatase in *Plasmodium falciparum*. *FEBS Lett* **460**(2): 217-220.

Lv, S., Zhang, K., Gao, Q., Lian, L., Song, Y. and Zhang, J. (2008). Overexpression of an H^+-PPase gene from *Thellungiella halophila* in cotton enhances salt tolerance and improves growth and photosynthetic performance. *Plant Cell Physiol* **49**(8): 1150-1164.

Maeshima, M. and Yoshida, S. (1989). Purification and properties of vacuolar membrane proton-translocating inorganic pyrophosphatase from mung bean. *J Biol Chem* **264**(33): 20068-20073.

Maeshima, M. (1990). Oligomeric structure of H(+)-translocating inorganic pyrophosphatase of plant vacuoles. *Biochem Biophys Res Commun* **168**(3): 1157-1162.

Maeshima, M. (2000). Vacuolar H(+)-pyrophosphatase. *Biochim Biophys Acta* **1465**(1-2): 37-51.

Martinez, R., Wang, Y., Benaim, G., Benchimol, M., de Souza, W., Scott, D.A. and Docampo, R. (2002). A proton pumping pyrophosphatase in the Golgi apparatus and plasma membrane vesicles of *Trypanosoma cruzi*. *Mol Biochem Parasitol* **120**(2): 205-213.

Martinoia, E., Maeshima, M. and Neuhaus, H.E. (2007). Vacuolar transporters and their essential role in plant metabolism. *J Exp Bot* **58**(1): 83-102.

Maruyama, C., Tanaka, Y., Takeyasu, K., Yoshida, M. and Sato, M.H. (1998). Structural studies of the vacuolar H(+)-pyrophosphatase: sequence analysis and identification of the residues modified by fluorescent cyclohexylcarbodiimide and maleimide. *Plant Cell Physiol* **39**(10): 1045-1053.

Matsushita, K. and Kaback, H.R. (1986). D-lactate oxidation and generation of the proton electrochemical gradient in membrane vesicles from *Escherichia coli* GR19N and in proteoliposomes reconstituted with purified D-lactate dehydrogenase and cytochrome o oxidase. *Biochemistry* **25**(9): 2321-2327.

McIntosh, M.T., Drozdowicz, Y.M., Laroiya, K., Rea, P.A. and Vaidya, A.B. (2001). Two classes of plant-like vacuolar-type H(+)-pyrophosphatases in malaria parasites. *Mol Biochem Parasitol* **114**(2): 183-195.

Mimura, H., Nakanishi, Y., Hirono, M. and Maeshima, M. (2004). Membrane topology of the H^+-pyrophosphatase of *Streptomyces coelicolor* determined by cysteine-scanning mutagenesis. *J Biol Chem* **279**(33): 35106-35112.

Mimura, H., Nakanishi, Y. and Maeshima, M. (2005a). Disulfide-bond formation in the H^+-pyrophosphatase of *Streptomyces coelicolor* and its implications for redox control and enzyme structure. *FEBS Lett* **579**(17): 3625-3631.

Mimura, H., Nakanishi, Y. and Maeshima, M. (2005b). Oligomerization of H(+)-pyrophosphatase and its structural and functional consequences. *Biochim Biophys Acta* **1708**(3): 393-403.

Miroux, B. and Walker, J.E. (1996). Over-production of proteins in *Escherichia coli*: mutant hosts that allow synthesis of some membrane proteins and globular proteins at high levels. *J Mol Biol* **260**(3): 289-298.

Mitsuda, N., Enami, K., Nakata, M., Takeyasu, K. and Sato, M.H. (2001). Novel type *Arabidopsis thaliana* H(+)-PPase is localized to the Golgi apparatus. *FEBS Lett* **488**(1-2): 29-33.

Motta, L.S., da Silva, W.S., Oliveira, D.M., de Souza, W. and Machado, E.A. (2004). A new model for proton pumping in animal cells: the role of pyrophosphate. *Insect Biochem Mol Biol* **34**(1): 19-27.

Motta, L.S., Ramos, I.B., Gomes, F.M., de Souza, W., Champagne, D.E., Santiago, M.F., Docampo, R., Miranda, K. and Machado, E.A. (2009). Proton-pyrophosphatase and polyphosphate in acidocalcisome-like vesicles from oocytes and eggs of *Periplaneta americana*. *Insect Biochem Mol Biol* **39**(3): 198-206.

Moyle, J., Mitchell, R. and Mitchell, P. (1972). Proton-translocating pyrophosphatase of *Rhodospirillum rubrum*. *FEBS Lett* **23**(2): 233-236.

Mulkidjanian, A.Y., Dibrov, P. and Galperin, M.Y. (2008). The past and present of sodium energetics: may the sodium-motive force be with you. *Biochim Biophys Acta* **1777**(7-8): 985-992.

Nakanishi, Y. and Maeshima, M. (1998). Molecular cloning of vacuolar H(+)-pyrophosphatase and its developmental expression in growing hypocotyl of mung bean. *Plant Physiol* **116**(2): 589-597.

Nakanishi, Y., Saijo, T., Wada, Y. and Maeshima, M. (2001). Mutagenic analysis of functional residues in putative substrate-binding site and acidic domains of vacuolar H^+-pyrophosphatase. *J Biol Chem* **276**(10): 7654-7660.

Nakanishi, Y., Yabe, I. and Maeshima, M. (2003). Patch clamp analysis of a H^+-pump heterologously expressed in giant yeast vacuoles. *J Biochem (Tokyo)* **134**(4): 615-623.

Nore, B.F., Sakai, Y. and Baltscheffsky, M. (1990). Comparison of the contribution from different energy-linked reactions to the function of a membrane-potential in photosynthetic bacteria. *Biochim Biophys Acta* **1015**(2): 189-194.

Nyren, P., Hajnal, K. and Baltscheffsky, M. (1984). Purification of the membrane-bound proton-translocating inorganic pyrophosphatase from *Rhodospirillum rubrum*. *Biochim Biophys Acta* **766**(3): 630-635.

Nyren, P. and Lundin, A. (1985). Enzymatic method for continuous monitoring of inorganic pyrophosphate synthesis. *Anal Biochem* **151**(2): 504-509.

Nyren, P., Nore, B.F. and Baltscheffsky, M. (1986). Studies on photosynthetic inorganic pyrophosphate formation in *Rhodospirillum rubrum* chromatophores. *Biochim Biophys Acta* **851**(2): 276-282.

Nyren, P., Nore, B.F. and Strid, A. (1991). Proton-pumping *N*,*N*'-dicyclohexylcarbodiimide-sensitive inorganic pyrophosphate synthase from *Rhodospirillum rubrum*: purification, characterization, and reconstitution. *Biochemistry* **30**(11): 2883-2887.

Nyren, P. and Strid, Å. (1991). Hypothesis: the physiological role of the membrane-bound proton-translocating pyrophosphatase in some phototrophic bacteria. *FEMS Microbiol Lett* **77**(2-3): 265-270.

Oberbeck, K., Drucker, M. and Robinson, D.G. (1994). V-type ATPase and pyrophosphatase in endomembranes of maize roots. *J Exp Bot* **45**(2): 235-244.

Obermeyer, G., Sommer, A. and Bentrup, F.W. (1996). Potassium and voltage dependence of the inorganic pyrophosphatase of intact vacuoles from *Chenopodium rubrum*. *Biochim Biophys Acta* **1284**(2): 203-212.

Ordaz, H., Sosa, A., Romero, I. and Celis, H. (1992). Thermostability and activation by divalent-cations of the membrane-bound inorganic pyrophosphatase of *Rhodospirillum rubrum*. *Int J Biochem* **24**(10): 1633-1638.

Palma, D.A., Blumwald, E. and Plaxton, W.C. (2000). Upregulation of vacuolar H(+)-translocating pyrophosphatase by phosphate starvation of *Brassica napus* (rapeseed) suspension cell cultures. *FEBS Lett* **486**(2): 155-158.

Park, S., Li, J., Pittman, J.K., Berkowitz, G.A., Yang, H., Undurraga, S., Morris, J., Hirschi, K.D. and Gaxiola, R.A. (2005). Up-regulation of a H^+-pyrophosphatase (H^+-PPase) as a strategy to engineer drought-resistant crop plants. *Proc Natl Acad Sci U S A* **102**(52): 18830-18835.

Perez-Castineira, J.R., Lopez-Marques, R.L., Losada, M. and Serrano, A. (2001). A thermostable K(+)-stimulated vacuolar-type pyrophosphatase from the hyperthermophilic bacterium *Thermotoga maritima*. *FEBS Lett* **496**(1): 6-11.

Perez-Castineira, J.R., Alvar, J., Ruiz-Perez, L.M. and Serrano, A. (2002a). Evidence for a wide occurrence of proton-translocating pyrophosphatase genes in parasitic and free-living protozoa. *Biochem Biophys Res Commun* **294**(3): 567-573.

Perez-Castineira, J.R., Lopez-Marques, R.L., Villalba, J.M., Losada, M. and Serrano, A. (2002b). Functional complementation of yeast cytosolic pyrophosphatase by bacterial and plant H^+-translocating pyrophosphatases. *Proc Natl Acad Sci U S A* **99**(25): 15914-15919.

Pisa, K.Y., Weidner, C., Maischak, H., Kavermann, H. and Muller, V. (2007). The coupling ion in the methanoarchaeal ATP synthases: H(+) vs. Na(+) in the A(1)A(o) ATP synthase from the archaeon *Methanosarcina mazei* Go1. *FEMS Microbiol Lett* **277**(1): 56-63.

Pohjanjoki, P., Fabrichniy, I.P., Kasho, V.N., Cooperman, B.S., Goldman, A., Baykov, A.A. and Lahti, R. (2001). Probing essential water in yeast pyrophosphatase by directed mutagenesis and fluoride inhibition measurements. *J Biol Chem* **276**(1): 434-441.

Polvani, C. and Blostein, R. (1988). Protons as substitutes for sodium and potassium in the sodium pump reaction. *J Biol Chem* **263**(32): 16757-16763.

Rajagopal, L., Clancy, A. and Rubens, C.E. (2003). A eukaryotic type serine/threonine kinase and phosphatase in *Streptococcus agalactiae* reversibly phosphorylate an inorganic pyrophosphatase and affect growth, cell segregation, and virulence. *J Biol Chem* **278**(16): 14429-14441.

Randahl, H. (1979). Characterization of the membrane-bound inorganic pyrophosphatase in *Rhodospirillum rubrum*. *Eur J Biochem* **102**(1): 251-256.

Rao, P.V. and Keister, D.L. (1978). Energy-liked reactions in photosynthetic bacteria. X. Solubilization of the membrane-bound energy-linked inorganic pyrophosphatase of *Rhodospirillum rubrum*. *Biochem Biophys Res Commun* **84**(2): 465-473.

Ratajczak, R., Hinz, G. and Robinson, D.G. (1999). Localization of pyrophosphatase in membranes of *Cauliflower inflorescence* cells. *Planta* **208**(2): 205-211.

Rea, P.A. and Poole, R.J. (1985). Proton-translocating inorganic pyrophosphatase in red beet (*Beta vulgaris L.*) tonoplast vesicles. *Plant Physiol* **77**(1): 46-52.

Rea, P.A. and Poole, R.J. (1986). Chromatographic resolution of H^+-translocating pyrophosphatase from H^+-translocating ATPase of higher plant tonoplast. *Plant Physiol* **81**: 126-129.

Robinson, D.G., Haschke, H.-P., Hinz, G., Hoh, B., Maeshima, M. and Marty, F. (1996). Immunological detection of tonoplast polypeptides in the plasma membrane of pea cotyledons. *Planta (Heidelberg)* **198**(1): 95-103.

Robinson, D.G., Hoppenrath, M., Oberbeck, K., Luykx, P. and Ratajczak, R. (1998). Localization of pyrophosphatase and V-ATPase in *Chlamydomonas reinhardtii*. *Bot Acta* **111**(2): 108-122.

Rodrigues, C.O., Scott, D.A. and Docampo, R. (1999a). Characterization of a vacuolar pyrophosphatase in *Trypanosoma brucei* and its localization to acidocalcisomes. *Mol Cell Biol* **19**(11): 7712-7723.

Rodrigues, C.O., Scott, D.A. and Docampo, R. (1999b). Presence of a vacuolar H^+-pyrophosphatase in promastigotes of *Leishmania donovani* and its localization to a different compartment from the vacuolar H^+-ATPase. *Biochem J* **340**(Pt 3): 759-766.

Rodrigues, C.O., Scott, D.A., Bailey, B.N., De Souza, W., Benchimol, M., Moreno, B., Urbina, J.A., Oldfield, E. and Moreno, S.N. (2000). Vacuolar proton pyrophosphatase activity and pyrophosphate (PP_i) in *Toxoplasma gondii* as possible chemotherapeutic targets. *Biochem J* **349** (Pt 3): 737-745.

Romero, I., Gomezpriego, A. and Celis, H. (1991). A membrane-bound pyrophosphatase from respiratory membranes of *Rhodospirillum rubrum*. *J Gen Microbiol* **137**: 2611-2616.

Ronquist, F. and Huelsenbeck, J.P. (2003). MrBayes 3: Bayesian phylogenetic inference under mixed models. *Bioinformatics* **19**(12): 1572-1574.

Ros, R., Romieu, C., Gibrat, R. and Grignon, C. (1995). The plant inorganic pyrophosphatase does not transport K^+ in vacuole membrane vesicles multilabeled with fluorescent probes for H^+, K^+, and membrane potential. *J Biol Chem* **270**(9): 4368-4374.

Rosen, B.P. (1986). Ion extrusion systems in *Escherichia coli*. *Methods Enzymol* **125**: 328-336.

Ruiz, F.A., Marchesini, N., Seufferheld, M., Govindjee and Docampo, R. (2001). The polyphosphate bodies of *Chlamydomonas reinhardtii* possess a proton pumping pyrophosphatase and are similar to acidocalcisomes. *J Biol Chem* **276**(49): 46196-46203.

Saier, M.H., Jr. (2003). Tracing pathways of transport protein evolution. *Mol Microbiol* **48**(5): 1145-1156.

Sarafian, V. and Poole, R.J. (1989). Purification of an H^+-translocating inorganic pyrophosphatase from vacuole membranes of red beet. *Plant Physiology* **91**(1): 34-38.

Sarafian, V., Kim, Y., Poole, R.J. and Rea, P.A. (1992a). Molecular cloning and sequence of cDNA encoding the pyrophosphate-energized vacuolar membrane proton pump of *Arabidopsis thaliana*. *Proc Natl Acad Sci U S A* **89**(5): 1775-1779.

Sarafian, V., Potier, M. and Poole, R.J. (1992b). Radiation-inactivation analysis of vacuolar H^+-ATPase and H^+-pyrophosphatase from *Beta vulgaris L.* – functional sizes for substrate hydrolysis and for H^+ transport. *Biochem J* **283**: 493-497.

Sato, M.H., Maeshima, M., Ohsumi, Y. and Yoshida, M. (1991). Dimeric structure of H(+)-translocating pyrophosphatase from pumpkin vacuolar membranes. *FEBS Lett* **290**(1-2): 177-180.

Sato, M.H., Kasahara, M., Ishii, N., Homareda, H., Matsui, H. and Yoshida, M. (1994). Purified vacuolar inorganic pyrophosphatase consisting of a 75-kDa polypeptide can pump H^+ into reconstituted proteoliposomes. *J Biol Chem* **269**(9): 6725-6728.

Schmidt, A.L. and Briskin, D.P. (1993). Energy transduction in tonoplast vesicles from red beet (*Beta vulgaris L.*) storage tissue: H^+/substrate stoichiometries for the H(+)-ATPase and H(+)-PPase. *Arch Biochem Biophys* **301**(1): 165-173.

Schultz, A. and Baltscheffsky, M. (2003). Properties of mutated *Rhodospirillum rubrum* H^+-pyrophosphatase expressed in *Escherichia coli*. *Biochim Biophys Acta* **1607**(2-3): 141-151.

Schultz, A. and Baltscheffsky, M. (2004). Inhibition studies on *Rhodospirillum rubrum* H(+)-pyrophosphatase expressed in *Escherichia coli*. *Biochim Biophys Acta* **1656**(2-3): 156-165.

Schultz, J.E. and Weaver, P.F. (1982). Fermentation and anaerobic respiration by *Rhodospirillum rubrum* and *Rhodopseudomonas capsulata*. *J Bacteriol* **149**(1): 181-190.

Scott, D.A., de Souza, W., Benchimol, M., Zhong, L., Lu, H.G., Moreno, S.N. and Docampo, R. (1998). Presence of a plant-like proton-pumping pyrophosphatase in acidocalcisomes of *Trypanosoma cruzi*. *J Biol Chem* **273**(34): 22151-22158.

Serrano, A., Perez-Castineira, J.R., Baltscheffsky, H. and Baltscheffsky, M. (2004). Proton-pumping inorganic pyrophosphatases in some archaea and other extremophilic prokaryotes. *J Bioenerg Biomembr* **36**(1): 127-133.

Serrano, A., Perez-Castineira, J.R., Baltscheffsky, M. and Baltscheffsky, H. (2007). H^+-PPases: yesterday, today and tomorrow. *IUBMB Life* **59**(2): 76-83.

Seufferheld, M., Vieira, M.C., Ruiz, F.A., Rodrigues, C.O., Moreno, S.N. and Docampo, R. (2003). Identification of organelles in bacteria similar to acidocalcisomes of unicellular eukaryotes. *J Biol Chem* **278**(32): 29971-29978.

Seufferheld, M., Lea, C.R., Vieira, M., Oldfield, E. and Docampo, R. (2004). The H(+)-pyrophosphatase of *Rhodospirillum rubrum* is predominantly located in polyphosphate-rich acidocalcisomes. *J Biol Chem* **279**(49): 51193-51202.

Seufferheld, M.J., Alvarez, H.M. and Farias, M.E. (2008). Role of polyphosphates in microbial adaptation to extreme environments. *Appl Environ Microbiol* **74**(19): 5867-5874.

Shakhov, Y.A., Nyren, P. and Baltscheffsky, M. (1982). Reconstitution of highly purified proton-translocating pyrophosphatase from *Rhodospirillum rubrum*. *FEBS Lett* **146**(1): 177-180.

Shimmen, T. and MacRobbie, E.A.C. (1987). Characterization of two proton transport systems in the tonoplast of plasmalemma-permeabilized nitella cells. *Plant Cell Physiol* **28**(6): 1023-1061.

Shintani, T., Uchiumi, T., Yonezawa, T., Salminen, A., Baykov, A.A., Lahti, R. and Hachimori, A. (1998). Cloning and expression of a unique inorganic pyrophosphatase from *Bacillus subtilis*: evidence for a new family of enzymes. *FEBS Lett* **439**(3): 263-266.

Shiratake, K., Kanayama, Y., Maeshima, M. and Yamaki, S. (1997). Changes in H(+)-pumps and a tonoplast intrinsic protein of vacuolar membranes during the development of pear fruit. *Plant Cell Physiol* **38**(9): 1039-1045.

Smirnova, I.N., Kudryavtseva, N.A., Komissarenko, S.V., Tarusova, N.B. and Baykov, A.A. (1988). Diphosphonates are potent inhibitors of mammalian inorganic pyrophosphatase. *Arch Biochem Biophys* **267**(1): 280-284.

Sosa, A., Ordaz, H., Romero, I. and Celis, H. (1992). Mg^{2+} is an essential activator of hydrolytic activity of membrane-bound pyrophosphatase of *Rhodospirillum rubrum*. *Biochem J* **283**: 561-566.

Sosa, A. and Celis, H. (1995). H^+/PP_i stoichiometry of membrane-bound pyrophosphatase of *Rhodospirillum rubrum*. *Arch Biochem Biophys* **316**(1): 421-427.

Stemmer, W.P. and Morris, S.K. (1992). Enzymatic inverse PCR: a restriction site independent, single-fragment method for high-efficiency, site-directed mutagenesis. *Biotechniques* **13**(2): 214-220.

Strid, Å., Karlsson, I.-M. and Baltcheffsky, M. (1987). Demonstration of ΔpH- and Δψ-induced synthesis of inorganic pyrophosphate in chromatophores from *Rhodospirillum rubrum*. *FEBS Lett* **224**(2): 348-352.

Suzuki, K. and Kasamo, K. (1993). Effects of aging on the ATP-dependent and pyrophosphate-dependent pumping of protons across the tonoplast isolated from pumpkin cotyledons. *Plant Cell Physiol* **34**(4): 613-619.

Suzuki, Y., Kanayama, Y., Shiratake, K. and Yamaki, S. (1999). Vacuolar H^+-pyrophosphatase purified from pear fruit. *Phytochemistry* **50**(4): 535-539.

Thompson, J.D., Gibson, T.J., Plewniak, F., Jeanmougin, F. and Higgins, D.G. (1997). The CLUSTAL X windows interface: flexible strategies for multiple sequence alignment aided by quality analysis tools. *Nucleic Acids Res* **25**(24): 4876-4882.

Tzeng, C.M., Yang, C.Y., Yang, S.J., Jiang, S.S., Kuo, S.Y., Hung, S.H., Ma, J.T. and Pan, R.L. (1996). Subunit structure of vacuolar proton-pyrophosphatase as determined by radiation inactivation. *Biochem J* **316**(Pt 1): 143-147.

Ueda, A., Kathiresan, A., Bennett, J. and Takabe, T. (2006). Comparative transcriptome analyses of barley and rice under salt stress. *Theor Appl Genet* **112**(7): 1286-1294.

Urbina, J.A., Moreno, B., Vierkotter, S., Oldfield, E., Payares, G., Sanoja, C., Bailey, B.N., Yan, W., Scott, D.A., Moreno, S.N. and Docampo, R. (1999). Trypanosoma cruzi contains major pyrophosphate stores, and its growth *in vitro* and *in vivo* is blocked by pyrophosphate analogs. *J Biol Chem* **274**(47): 33609-33615.

Van, R.C., Pan, Y.J., Hsu, S.H., Huang, Y.T., Hsiao, Y.Y. and Pan, R.L. (2005). Role of transmembrane segment 5 of the plant vacuolar H+-pyrophosphatase. *Biochim Biophys Acta* **1709**(1): 84-94.

Waggoner, A.S. (1979). Dye indicators of membrane potential. *Annu Rev Biophys Bioeng* **8**: 47-68.

Walker, R.R. and Leigh, R.A. (1981). Mg^{2+}-dependent, cation-stimulated inorganic pyrophosphatase associated with vacuoles isolated from storage roots of red beet. *Planta* **153**: 150-155.

Wang, Y., Leigh, R.A., Kaestner, K.H. and Sze, H. (1986). Electrogenic H^+-pumping pyrophosphatase in tonoplast vesicles of oat roots. *Plant Physiol* **81**(2): 497-502.

Wanger, G.J. and Mulready, P. (1983). Characterization and solubilization of nucleotide-specific Mg^{2+}-ATPase and Mg^{2+}-pyrophosphatase of tonoplast. *Biochim Biophys Acta* **728**: 267-280.

White, P.J., Marshall, J. and Smith, J.A.C. (1990). Substrate kinetics of the tonoplast H^+-translocating inorganic pyrophosphatase and its activation by free Mg^{2+}. *Plant Physiol* **93**(3): 1063-1070.

Wu, J.J., Ma, J.T. and Pan, R.L. (1991). Functional size analysis of pyrophosphatase from *Rhodospirillum rubrum* determined by radiation inactivation. *FEBS Lett* **283**(1): 57-60.

Yang, H., Knapp, J., Koirala, P., Rajagopal, D., Peer, W.A., Silbart, L.K., Murphy, A. and Gaxiola, R.A. (2007). Enhanced phosphorus nutrition in monocots and dicots over-expressing a phosphorus-responsive type I H(+)-pyrophosphatase. *Plant Biotechnol J* **5**(6): 735-745.

Yang, S.J., Ko, S.J., Tsai, Y.R., Jiang, S.S., Kuo, S.Y., Hung, S.H. and Pan, R.L. (1998). Subunit interaction of vacuolar H^+-pyrophosphatase as determined by high hydrostatic pressure. *Biochem J* **331**(Pt 2): 395-402.

Yang, S.J., Jiang, S.S., Kuo, S.Y., Hung, S.H., Tam, M.F. and Pan, R.L. (1999). Localization of a carboxylic residue possibly involved in the inhibition of vacuolar H^+-pyrophosphatase by *N*, *N*'-dicyclohexylcarbodi-imide. *Biochem J* **342**(Pt 3): 641-646.

Yang, S.J., Jiang, S.S., Van, R.C., Hsiao, Y.Y. and Pan, R. (2000). A lysine residue involved in the inhibition of vacuolar H(+)-pyrophosphatase by fluorescein 5'-isothiocyanate. *Biochim Biophys Acta* **1460**(2-3): 375-383.

Yang, S.J., Jiang, S.S., Hsiao, Y.Y., Van, R.C., Pan, Y.J. and Pan, R.L. (2004). Thermoinactivation analysis of vacuolar H(+)-pyrophosphatase. *Biochim Biophys Acta* **1656**(2-3): 88-95.

Young, T.W., Kuhn, N.J., Wadeson, A., Ward, S., Burges, D. and Cooke, G.D. (1998). *Bacillus subtilis* ORF yybQ encodes a manganese-dependent inorganic pyrophosphatase with distinctive properties: the first of a new class of soluble pyrophosphatase? *Microbiology* **144**(Pt 9): 2563-2571.

Zancani, M., Skiera, L.A. and Sanders, D. (2007). Roles of basic residues and salt-bridge interaction in a vacuolar H^+-pumping pyrophosphatase (AVP1) from *Arabidopsis thaliana*. *Biochim Biophys Acta* **1768**(2): 311-316.

Zeng, R., Duan, C., Li, X., Tian, W. and Nie Z. (2009). Vacuolar-type inorganic pyrophosphatase located on the rubber particle in the latex is an essential enzyme in regulation of the rubber biosynthesis in *Hevea brasiliensis*. *Plant Science* **176**(5): 602-607.

Zhang, Y.Y., Wang, L.L., Liu, Y.L., Zhang, Q., Wei, Q.P. and Zhang, W.H. (2006). Nitric oxide enhances salt tolerance in maize seedlings through increasing activities of proton-pump and Na^+/H^+ antiport in the tonoplast. *Planta* **224**(3): 545-555.

Zhao, F.Y., Zhang, X.J., Li, P.H., Zhao, Y.X. and Zhang, H. (2006). Co-expression of the *Suaeda salsa* SsNHX1 and Arabidopsis AVP1 confer greater salt tolerance to transgenic rice than the single SsNHX1. *Molecular Breeding* **17**(4): 341-353.

Zhen, R.G., Baykov, A.A., Bakuleva, N.P. and Rea, P.A. (1994a). Aminomethylenediphosphonate: a potent type-specific inhibitor of both plant and phototrophic bacterial H^+-pyrophosphatases. *Plant Physiol* **104**(1): 153-159.

Zhen, R.G., Kim, E.J. and Rea, P.A. (1994b). Localization of cytosolically oriented maleimide-reactive domain of vacuolar H(+)-pyrophosphatase. *J Biol Chem* **269**(37): 23342-23350.

Zhen, R.G., Kim, E.J. and Rea, P.A. (1997). Acidic residues necessary for pyrophosphate-energized pumping and inhibition of the vacuolar H^+-pyrophosphatase by *N*,*N*'-dicyclohexylcarbodiimide. *J Biol Chem* **272**(35): 22340-22348.

Zingarelli, L., Anzani, P. and Lado, P. (1994). Enhanced K^+-stimulated pyrophosphatase activity in NaCl-adapted cells of *Acer pseudoplatanus*. *Physiologia Plantarum* **91**(3): 510-516.

Zyryanov, A.B., Vener, A.V., Salminen, A., Goldman, A., Lahti, R. and Baykov, A.A. (2004). Rates of elementary catalytic steps for different metal forms of the family II pyrophosphatase from *Streptococcus gordonii*. *Biochemistry* **43**(4): 1065-1074.